Institut für Thermodynamik und Reaktionstechnik
Technische Universität Berlin
ERASMUS/SOKRATES-Programm 1997/98

Supervisor: Dr. Lennart Vamling

Examinator: Prof. Thore Berntsson

Göteborg, 20. Juni 1998

Performance Comparison of Evaporator Tubes with a Star-shaped Insert

Sven Wellsandt

Abstract

When producing chillers for cruiser ships, the necessity of space-saving design is the main reason for the use of evaporator tubes with a star-shaped insert, as they offer an refrigerant side area enhancement of about a factor three.

This project was initiated by **Sabroe Refrigeration AB** who produce the above mentioned chillers. They received tube samples from two potential manufacturers and wanted to decide which of them they might use in their future production. It was felt that a single tube comparison would enable the required information about a possible difference of heat transfer between the tubes.

In the experimental part of the project an existing facility was used which had been constructed over several years to make a controlled investigation of horizontal evaporator tubes possible. At this facility, the test section was modified to enable global measurements for the two tubes and to closely resemble the conditions in a large scale evaporator.

For most experiments superheat conditions between 8 °C and 10 °C were chosen. To cover different flow regions the brine inlet temperature was varied between 8 °C, 10 °C and 12 °C. Conditions where incomplete evaporation occurs were also investigated.

A general superior performance of one tube could not be proved. At the lower end of the investigated flow region one tube showed better performance, whereas the other tube was better at higher flows. Possible causes of the different behaviour such as insert-shell connection, flow distribution and surface structure are discussed.

The second part of this project involved the comparison of experimental data with results from a simulation program used in the Department of Heat and Power Technology. The simulation program uses heat transfer correlations developed for smooth evaporator tubes which were adjusted for the different geometry of the tubes with inserts.

Calculated heat transfer data had to be corrected by a factor of 0.5 to 0.7 to fit to the experimental values depending on the heat transfer correlation chosen. In comparison the pressure drop calculations correlated to the measured data to within 5-10%.

It is suggested that the large deviation between measured and calculated data is due to the extended area of intermittently dry tube wall. Here the correlations applied might overestimate the heat transfer.

Zusammenfassung

Bei der Produktion von Kühlsystemen für den Schiffsverkehr ist das beschränkte Platzangebot für die Installation auschlaggebend für die Nutzung von Verdampferrohren mit sternförmigen Einbauten. Diese bieten im Vergleich zu Verdampferrohren ohne Einbauten einen internen Flächengewinn um einen Faktor drei.

Das vorliegende Projekt wurde iniziiert von **Sabroe Refrigeration AB**, die unter anderem die oben erwähnten Kühlsysteme mit den dazugehörigen Rohrbündel-Wärmeübertragern herstellen. Wärmeübertrager mit Verdampferrohren zweier potentieller Anbieter wurden von **Sabroe Refrigeration AB** getestet und signifikante Unterschiede in ihrer Leistung festgestellt. Ein vergleichender Test von Einzelrohren sollte nun Aufschluß über mögliche Unterschiede bei der Wärmeübertragung in den jeweiligen Rohren geben.

Im experimentellen Teil der Arbeite wurde eine in mehreren Jahren entwickelte Anlage genutzt, die eine kontrollierte Untersuchung von horizontalen Verdampferrohren ermöglicht. Die Meßtrecke dieser Anlage wurde während dieses Projektes komplett umgebaut, um einerseits globale Messungen am Rohr zu ermöglichen und andererseits den Zulaufbedingungen in den getesteten Rohbündel-Wärmeübertragern möglichst nahe zu kommen.

Getestet wurden sowohl Überhitzungsbedingungen zwischen 8-10 °C bei Wassertemperaturen von 8 °C, 10 °C und 12 °C als auch Bedingungen unvollständiger Verdampfung.

Eine durchgehend bessere Leistung eines der beiden Verdampferrohre konnte nicht festgestellt werden. Bei niedrigeren und höheren Massenströmen zeigte jeweils ein anderes Rohr bessere Leistung. Mögliche Ursachen für dieses unterschiedliche Verhalten, wie der Kontakt zwischen Einbauten und Rohr, unterschiedliche Verteilung des Kältemittels und Ober- flächenstruktur, werden diskutiert.

Im zweiten Teil der Arbeit werden die gemessenen Daten mit verschiedenen Korrelationen für Wärmeübergang und Druckverlust verglichen. Diese Korrelationen wurden in früheren Studien mittels Messungen an Rohren ohne Einbauten erstellt und später zwecks Anwendbarkeit für Rohre mit Einbauten um deren spezifischen geometrischen Parameter ergänzt.

Berechnete Wärmedurchgangskoeffizienten waren je nach verwendeter Gleichung 30-50% höher als die gemessenen Werte. Die Abweichungen von berechneten Druckverlusten lagen dagegen zwischen 5-10%.

Es wird vermutet, daß bei den untersuchten Verdampferrohren Ringströmung mit teilweise trockener Rohrwand schon bei niedrigeren Dampfgehalten auftritt. In diesem Bereich ist es wahrscheinlich, daß die angewandten Korrelationen den inneren Wärmeübergangskoeffizienten zu hoch berechnen.

Contents

1. Introduction

1.1 Background

The subject of boiling under conditions of natural or forced convection is an extremely important one. The design of refrigeration and air-conditioning equipment, heat pumps, petrochemical plant reboilers and many other major items essential to chemical and power plants is dependent upon an extensive knowledge of the fluid dynamics and heat transfer processes that occur during convective evaporation.

The urgent requirements of various industries for cold water at 1 to 2 °C necessitated the design of an evaporator where refrigerant is boiled inside, to replace the flooded evaporator traditionally employed in water coolers. Additionally the energy conservation demands in industry have increased during recent years, altering the requirements for heat exchanger design. Hence there is a trend towards reducing the driving force of heat exchangers whilst increasing the heat exchanger area.

One way to increase the area of evaporator tubes is to apply various types of inserts. This project investigated evaporator tubes with a ten channel star-shaped insert. **Sabroe Refrigeration AB** approached the Department of Heat and Power Technology at Chalmers University of Technology with a concern over the different performance of two of the afore-mentioned evaporator tubes in their large scale tests. **Sabroe Refrigeration AB** is especially dependent on the use of evaporator tubes with star-shaped inserts in their production of chillers for cruiser ships. Since here the space for installation is restricted, the optimal design of evaporator tubes consists of a maximum evaporation area at minimum tube length. With an area enhancement of about a factor three, tubes with star-shaped inserts currently fulfil this need best.

Sabroe Refrigeration AB had tested evaporator tube from different potential suppliers and detected different performances during their large scale tests. They were interested in a single tube comparison in order to receive detailed information, which might be able to support the conclusion that the different manufacturing is the reason for a difference in performance.

The present project represents the beginning of an experimental series investigating evaporator tubes with inserts. Therefore it should give initial information about the most efficient tube for further studies.

1.2 Purpose

The main purpose of this project was therefore to obtain experimental data which would enable a comprehensive comparison of the two tubes. To achieve this purpose, a facility was used which had been designed and built up by *Melin* (1996) for the investigation of heat transfer and pressure drop in straight smooth tubes. During the project the test section of this facility has been modified to closely resemble a single tube in a direct-expansion evaporator.

Presently there are no heat transfer and pressure drop correlations available which are based on measurements on tubes with star-shaped inserts. The department's simulation program uses correlations which were developed with smooth tubes. Therefore to make these correlations applicable, the specific geometrical parameters of the tubes with inserts were added.

A second task of this project was to use the measured data as input for the simulation program and investigate the deviation between measured and calculated heat transfer and pressure drop.

The use of HCFC22 for the measurements may disturb the reader, since the ozone-depleting effect of HCFC22 is well known. **Sabroe Refrigeration AB's** full scale experience is based on the use of HCFC22 as working fluid, making its application for a single tube comparison unavoidable. Additionally HCFC22 is the most thoroughly investigated refrigerant and thus makes the use of it for test reasons very consistent.

This project was the beginning of a series of investigations, hence it was appropriate to produce a data base using HCFC22. In the future this data can be utilised for comparisons with substitutes like refrigerant mixtures or flammable substances such as propane or n-butane.

2. Fundamentals

The following chapter will review those fundamentals which describe the specific heat transfer problems of this work.

2.1 Heat transfer - the fundamental equations

Heat transfer from a hotter to a colder fluid through a tube wall results from the combination of heat transfer from fluid to wall, heat conduction through the wall and heat transfer from wall to fluid. For those phenomena equations (0.1) to (0.3) apply.

$$\dot{Q} = \alpha_O A_O \cdot (T_O - T_{WO}) \tag{0.1}$$

$$\dot{Q} = \frac{\lambda_m}{\delta} A_m \cdot (T_{WO} - T_{WI}) \tag{0.2}$$

$$\dot{Q} = \alpha_I A_I \cdot (T_{WI} - T_I) \tag{0.3}$$

The unknown wall temperatures in those three equations can now be eliminated and the definition of the overall heat transfer coefficient is achieved.

$$\dot{Q} = UA \cdot (T_O - T_I) \tag{0.4}$$

The direct relation between the important parameters of heat transfer and conduction and the overall heat transfer coefficient is shown in equation (0.5).

$$\frac{1}{UA} = \frac{1}{\alpha_O A_O} + \sum_i \frac{\delta_i}{\lambda_{mi} A_{mi}} + \frac{1}{\alpha_I A_I} \tag{0.5}$$

If heat is conducted through several layers of different materials, the heat conduction term in equation (0.5) has to be a sum. However, for a very small ratio δ/A_m and high conductivity this sum can be neglected.

In applications where evaporation occurs, many more variables influence the heat transfer and thus it is much more complicated to give equations for the calculation of heat transfer coeffi-

cients. Two of the main influencing factors are the mass flux and the vapour fraction including its distribution. For better understanding a brief description of flow patterns in heated horizontal tubes will be given.

2.2 Two-phase flow patterns in a heated horizontal tube

Flow patterns formed during the generation of vapour in heated horizontal tubes are influenced by departures from thermodynamic and hydrodynamic equilibrium. Asymmetric phase distribution and stratification introduce additional complications.

Figure 0-1 shows a schematic representation of the various flow patterns encountered for convective evaporation in horizontal tubes. The sequence of flow patterns shown correspond to a relatively low inlet velocity (< 1m/s) and feeding of liquid just below saturation temperature.

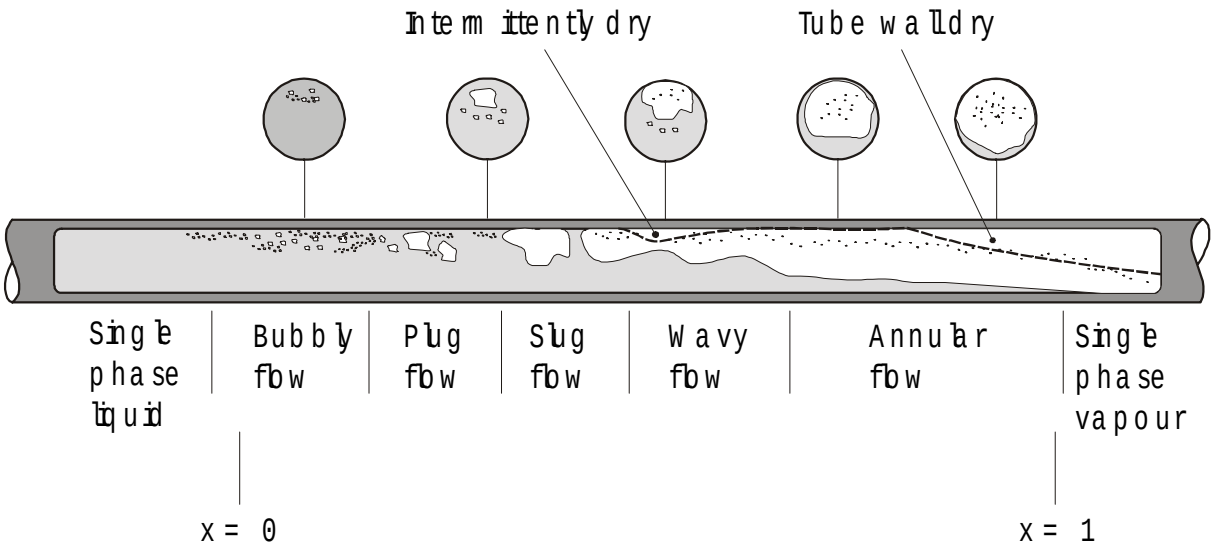

Figure 0-1 Two-phase flow patterns in a horizontal evaporator tube

As the vapour fraction increases the following flow patterns encounter in succession**:**

- *Single phase liquid*. No vapour fraction is existent.
- *Bubbly flow*. The pipe cross-section contains vapour bubbles which tend to travel in the upper half of the pipe.
- *Plug flow*. Vapour bubbles coalesce into plugs which again tend to travel in the upper half of the tube.
- *Wavy flow*. As the vapour velocity is increased the interface becomes disturbed by waves travelling in the direction of flow.

- *Annular flow*. A still higher vapour velocity will result in the formation of a gas core with a liquid film around the entire circumference (the film is thicker at the base of the pipe). The annular flow changes in the amount of dispersed liquid particles.
- *Single-phase vapour*. Eventually, when the annular flow disappears, little droplets travel through the tube which gradually evaporate.

Important points to note from a heat transfer viewpoint are the possibility of intermittent drying and rewetting of the upper surfaces of the tube in slug and wavy flow and the progressive drying out over long tube lengths of the upper circumference of the tube wall in annular flow.

In this work a tube with a ten channel insert was investigated. In each of those channels the flow patterns given above occur but might slightly differ due to specific surface structure and geometry. *D'Yachov* (1978) assumed that the boundaries between annular, dispersed annular and dispersed flows might shift towards smaller vapour fractions .

2.3 Convective evaporation

Convective evaporation is defined as being the addition of heat to a flowing liquid in such a way that generation of vapour occurs. This definition therefore excludes the process of flashing where vapour generation occurs solely as a result of reduction in system pressure. In many applications, however, the two processes do occur simultaneously and thus cannot be clearly separated.

Refering to Baehr and Stephan (1996), convective evaporation consists of two contributions, nucleate boiling and forced evaporation.

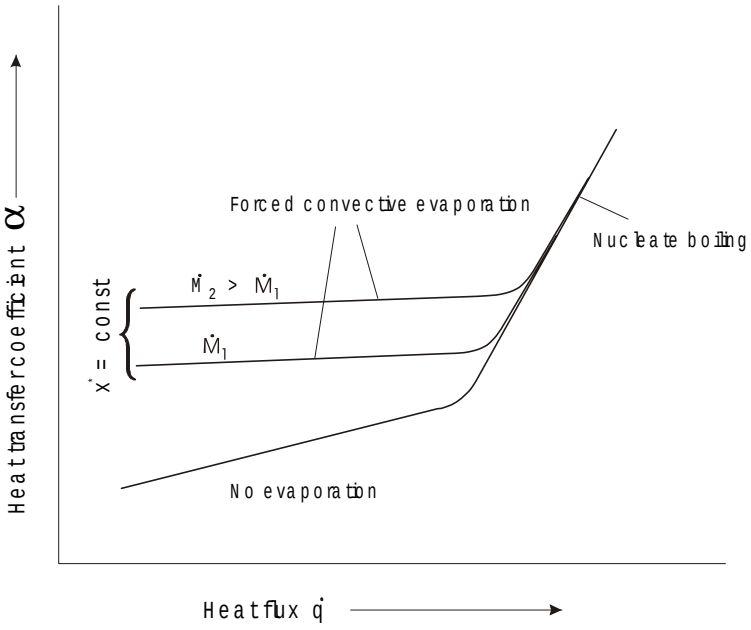

Figure 0-2 Heat transfer coefficient in nucleate boiling and forced convective evaporation

In the area of nucleate boiling the heat transfer coefficient depends mainly on the surface heat flux and hardly on the mass velocity whereas in the forced convective evaporation area the heat transfer is strongly determined by mass velocity or mass flux and little by the surface heat flux. This is shown in Figure 0-2 where the two areas are easily distinguished. A further independent variable is the vapour fraction $x^* = \dot{M}_V / \dot{M}$. With higher vapour fractions the curves in Figure 0-2 move towards greater heat transfer coefficients.

The heat transfer coefficient's dependence on the vapour fraction is shown in Figure 0-3. At lower vapour fractions nucleate boiling occurs and the heat transfer coefficient depends mainly on the heat flux. Further down stream the vapour fraction increases and hence its velocity as well. The heat input is mostly transferred to the liquid and vapour by convection. The greater forced convection results in reduction of wall superheat and suppression of nucleate boiling; at high mass fluxes even to such an extend that the suppression is complete.

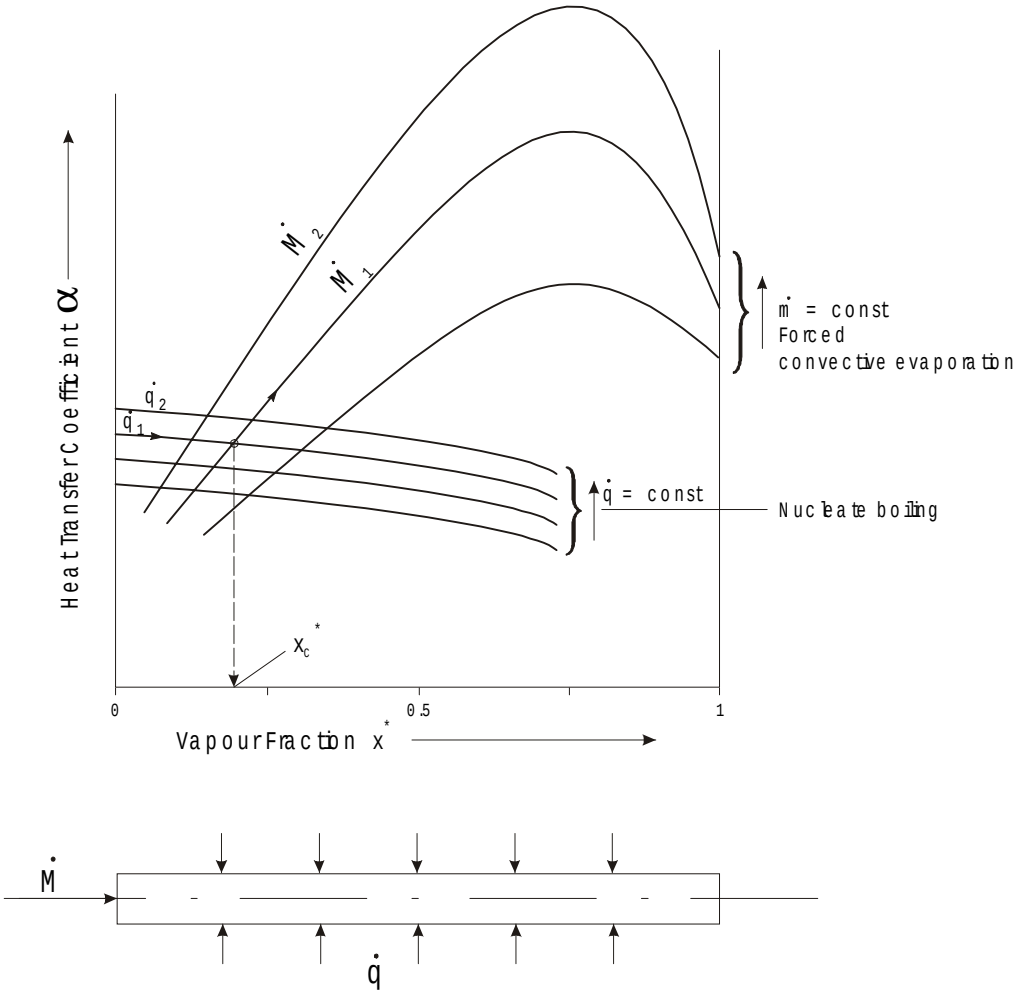

Figure 0-3 Curve of heat transfer coefficient for evaporation in a horizontal tube

When nucleate boiling changes into convective evaporation, the heat transfer coefficient is practically independent from heat flux and very dependent on mass flux and vapour fraction. At very large vapour fraction the heat transfer coefficient decreases due to the lower conductivity of vapour in comparison to liquid.

To calculate the heat transfer coefficient equations of the following form are used:

$$\alpha = c \cdot \dot{q}^n \cdot \dot{m}^s \cdot f(x^*) \qquad (0.6)$$

In equation (0.6) *c* is dependent on thermophysical substance properties. During convective convection, $n \approx 0$ whereas *s* varies between 0.6 and 0.8. In the area of nucleate boiling *n* becomes approximately ¾ and *s* varies between 0.1 and 0.3.

For a given application, the form of equation (0.6) also depends strongly on flow pattern.

2.4 Heat transfer correlations for convective evaporation using pure substances

There is still no general model to predict heat transfer in flow evaporation which proves the complexity of the task.

In the following section, we discuss correlations from the literature which the measured data were compared with. It has to be mentioned that the correlations were derived for convective evaporation in smooth tubes. To adapt the correlations for tubes with inserts the inner diameter has been replaced by the hydraulic diameter.

2.4.1 Pierre (1969)

The correlation of *Pierre* (1969) is a correlation widely used by the industry in Sweden and it is easy and accurate when used for conditions for which it was developed. It gives global values of heat transfer. However, in this work it has been applied locally. It has also been changed slightly, to reflect differences in transport property values between this and the original work. The modified Pierre correlation becomes:

$$Nu_{TP} = 0.00088\left(\mathrm{Re}_{lo}^{2}\, K_f\right)^{0.5} \tag{0.7}$$

where

$$K_f = \frac{\pi \dot{q}}{g \dot{m}} \tag{0.8}$$

2.4.2 Shah (1976)

Shah's correlation belongs to the group of enhancement models which are written as

$$\alpha_{TP} = \Psi \alpha_l \tag{0.9}$$

where Ψ is a two-phase multiplier modelling both the increased convective influence due to evaporation and nucleate boiling when the heat flux is large enough.

α_l is a single-phase forced convection equation calculated from the *Dittus and Boelter* (1985) correlation.

Shah (1979) developed a correlation where the two-phase multiplier Ψ was calculated from a chart. This chart used the boiling number *Bo*, the convection number *Co* and the Froude number *Fr* as parameters. Later *Shah* (1982) developed equations replacing the chart thus enabling the correlation to be programmed. However, the equations are a simplification of the chart and therefore do not correspond to it in every detail.

For horizontal flow and if the Froude number is less than 0.004

$$Co_{corr} = 0.38\, Co\, Fr^{-0,3} \tag{0.10}$$

For vertical and horizontal flow:

$$\begin{aligned} \Psi_l &= 230\ Bo^{0.5} && (\text{Bo} > 0.3 \cdot 10^{-4}) \\ \Psi_1 &= 1 + 46\, Bo^{0.5} && (\text{Bo} < 0.3 \cdot 10^{-4}) \end{aligned} \tag{0.11}$$

$$\begin{aligned} \Psi_2 &= C_1 \cdot Bo^{0.5} \cdot e^{2.74/Co^{0.1}} && (0.1 < \text{Co} < 1.0) \\ \Psi_2 &= C_1 \cdot Bo^{0.5} \cdot e^{2.74/Co^{0.15}} && (\text{Co} > 1.0 \end{aligned} \tag{0.12}$$

where

$$\begin{aligned} C_1 &= 14.7 && (\text{Bo} > 11 \cdot 10^{-4}) \\ C_1 &= 15.43 && (\text{Bo} < 11 \cdot 10^{-4}) \end{aligned} \tag{0.13}$$

$$\Psi_3 = 1.8/Co^{0.8} \tag{0.14}$$

$$\Rightarrow \qquad \Psi = Max(\Psi_1, \Psi_2, \Psi_3) \tag{0.15}$$

2.4.3 Klimenko (1988)

Klimenko's correlations as part of the asymptotic models divides the heat transfer into two separate parts. In the nucleate boiling region the heat transfer is little affected by forced convection and vice versa.

Klimenko (1988) defined three different heat transfer regions: two where the heat transfer is strongly dependent on evaporation and one where single-phase convection is dominant. Of the two evaporation regions, one is governed by nucleate boiling and one by forced convection.

For the nucleate boiling part he derived an equation based partly on the reasoning of *Styushin* (1977)

$$Nu_{NB} = 7.4 \cdot 10^{-3} Pe_{\mathrm{mod}}^{0.6} K_b^{0.5} \mathrm{Pr}_1^{-1/3} \left(\frac{\lambda_W}{\lambda_l} \right)^{0.15} \tag{0.16}$$

where the modified Péclet number is

$$Pe_{\mathrm{mod}} = \frac{\dot{q} b}{i_{fg} \rho_g a_l} \tag{0.17}$$

in which b is the Laplace constant and the dimensionless parameter K_b is

$$K_b = \frac{P}{\sqrt{\sigma g (\rho_l - \rho_g)}} \tag{0.18}$$

For the forced convection region he derived:

$$Nu_{FC} = 0.087 \, \mathrm{Re}_m^{0.6} \, \mathrm{Pr}_l^{1/6} \left(\frac{\rho_g}{\rho_l} \right)^{0.2} \left(\frac{\lambda_W}{\lambda_l} \right)^{0.09} \tag{0.19}$$

where the Reynolds number of two-phase mixtures is

$$\mathrm{Re}_m = \frac{w_m b}{\nu_l} \tag{0.20}$$

and the two-phase mixture velocity is

$$w_m = \left(\frac{G}{\rho_l} \right) \cdot \left[1 + x \left(\frac{\rho_l}{\rho_g} - 1 \right) \right] \tag{0.21}$$

To distinguish between the two regions he defined a convective boiling number

$$N_{CB} = \frac{\mathrm{Re}_m}{\mathrm{Re}_*} \cdot \left(\frac{\rho_l}{\rho_g} \right)^{2/3} \tag{0.22}$$

where the modified Reynolds number is defined as

$$\mathrm{Re}_{*} = \frac{\dot{q} b}{i_{fg} \rho_g \nu_l} \tag{0.23}$$

Klimenko (1988) found by comparing with experimental data that he could clearly distinguish between the two regions using the parameter N_{CB}. This led to the following correlation:

$$Nu_{TP} = \begin{pmatrix} Nu_{NB} & with & N_{CB} < 1.6 \cdot 10^4 \\ Nu_{FC} & with & N_{CB} > 1.6 \cdot 10^4 \end{pmatrix} \tag{0.24}$$

2.4.4 Melin (1996)

Melin (1996) developed a correlation which claims to be applicable to any substance that can be used in heat pump and refrigeration cycles.

The heat transfer coefficient for a pure substance is

$$\left(\alpha_{TP}\right)^{n(P_r)} = \left(E \cdot \alpha_l\right)^{n(P_r)} + \left(S \cdot \alpha_{NB}\right)^{n(P_r)} \tag{0.25}$$

where

$$E = 2.37 \cdot \left(0.29 + 1/X_{tt}\right)^{0.85} \tag{0.26}$$

$$\alpha_l = 0.023 \mathrm{Re}_l^{0.8} \mathrm{Pr}_l^{0.4} \cdot \lambda / d_h \tag{0.27}$$

$$S = 5.58 \cdot 10^{-2} \left(\frac{\mu_l}{\mu_g}\right)^{0.1} \left(\frac{d_b}{d_h} x\right)^{-0.285} \cdot \mathrm{Re}_m^{0.165} \tag{0.28}$$

$$\alpha_{NB} = 9.7 \cdot P_c^{0.5} F(P_r) \mathrm{Re}_b^{0.67} \mathrm{Pr}_l^{0.4} \cdot \lambda_l / d_h \tag{0.29}$$

$$F(P_r) = 1.8 P_r^{0.17} + 4 P_r^{1.2} + 10 P_r^{10} \tag{0.30}$$

$$n\left(P_r\right) = 40.8 \cdot P_r^{0.85} \tag{0.31}$$

X_{tt} is the Martinelli parameter and is defined as

$$X_{tt} = \left[(1-x)/x\right]^{0.9} \cdot (\rho_g / \rho_l)^{0.5} \cdot \left(\mu_l / \mu_g\right)^{0.1} \qquad (0.32)$$

2.5 Dry-wall convection

As the vapour quality increases along the tube, a stage is reached when the rate of deposition of mist on the heated surface is less than the potential rate of evaporation; so the wall becomes dry. Consequently the heat is transferred just by single-phase convection in the vapour, which is less than in the liquid at the same mass flow rate. The vapour becomes superheated and the remaining mist evaporates as a result of transfer of heat from vapour to droplets.

The main mechanism of heat transfer is likely to be by convection from the heated wall to the superheated vapour. This can be estimated by the normal method of calculating single-phase heat transfer (see below), if the amount of superheat is assumed to be negligible. This is the method normally adopted for a rough estimate, but it is liable to overestimate the heat flux, because there is usually an appreciable amount of superheat of the vapour, the amount being difficult to estimate.

2.5.1 Heat transfer correlation for single-phase flow

In applications where superheat occurs a correlation for single-phase flow has to be used for the superheat part. This could be the one which is currently used in the Department of Heat and Power Technology and recommended by *ESDU* (1967):

$$Nu = 0.02246\,\mathrm{Re}^{0.794}\ \mathrm{Pr}^{(0.495-0.0225\ln \mathrm{Pr})} \qquad (0.33)$$

2.6 Heat transfer in a concentric annulus for turbulent flow[1]

For an arrangement where heat is transferred to the inner tube and the outer tube is insulated (see Figure 3-2), the heat transfer is described by a modified form of the equation for straight tubes

$$\frac{Nu}{Nu_{tube}} = f\left(d_i/d_a\right) \qquad (0.34)$$

[1] VDI-Wärmeatlas (1988)

Petukhov and *Roizen* (1964) found for the function on the right side of equation (0.34)

$$\frac{Nu}{Nu_{tube}} = 0.86\left(d_a/d_i\right)^{0.16} \tag{0.35}$$

Nu_{tube} can be calculated by *Gnielinski's* (1975) correlation which also covers the transition zone between laminar and turbulent flow. Herein the hydraulic diameter d_h has to be substituted for the inner diameter d_i.

$$Nu_{tube} = \frac{\xi/8\cdot(\mathrm{Re}-1000)\,\mathrm{Pr}}{1+12.7\cdot\sqrt{\xi/8}\cdot\left(\mathrm{Pr}^{2/3}-1\right)}\left[1+\left(\frac{d_h}{l}\right)^{2/3}\right] \tag{0.36}$$

where

$$\xi = \left(1.82\log_{10}\mathrm{Re}-1.64\right)^{-2} \tag{0.37}$$

$$d_h = d_a - d_i \tag{0.38}$$

Now the Nu number in equation (0.35) can be calculated and the outer heat transfer coefficient is achieved by

$$Nu = \frac{\alpha_O \cdot d_h}{\lambda} \tag{0.39}$$

The region of validity is

$$\mathrm{Re} = \frac{w\,d_h}{\nu} > 2300 \quad \text{to} \quad \mathrm{Re} = 10^6 \tag{0.40}$$

$$\mathrm{Pr} = 0.6 \text{ to } \mathrm{Pr} = 1000 \tag{0.41}$$

$$d_h/l = 0 \text{ to } d_h/l = 1 \tag{0.42}$$

2.7 Pressure drop correlations for non-adiabatic two-phase flow

Measured data was compared to two pressure drop correlations which are shown below. For detailed theoretical explanation of the basic concepts of pressure drop modelling one may refer to *Collier* (1994).

2.7.1 Pierre (1957)

Pierre (1957) derived his correlation in conditions close to the ones of this investigation. They are shown in Table 0-1.

He derived an equation that would predict both the frictional pressure drop and the acceleration pressure drop. From an energy equation *Pierre* (1957) obtained the following expression for the pressure drop in an evaporator of length L:

$$\frac{-dp_{TP}}{L} = \left[f_m + \frac{x_2 - x_1}{x_m} \cdot \frac{d_h}{L} \right] \cdot G^2 \nu_m / d_h \qquad (0.43)$$

where, for the case when Re K_f >1,

$$f_m = 0.0185 K_f^{1/4} \cdot \mathrm{Re}_{lo}^{-1/4} \qquad (0.44)$$

in which K_f is *Pierre's* boiling number, defined by equation (0.8).

Table 0-1 Experimental conditions for Pierre and this investigation

	PIERRE	THIS INVESTIGATION
Working media	R12, R22, R502	R22
Length of evaporator (m)	4.08 - 9.50	4.00
Mass flow (g/s)	4 - 40	14 - 36
Heat flux (W/m^2)	1100 - 30000	3300 - 7900
Evaporation temperature (°C)	- 20 to + 10	-2.5 to +2.5
Inlet vapour quality	0.10 - 0.20	0.13 - 0.14
Outlet condition	5 to 7 degrees superheat	8 to 10.5 degrees superheat
Evaporator diameter (mm)	12 and 18	17.5

2.7.2 Chawla (1967) and Bankoff (1960)

Chawla (1967) suggested the following model:

$$-\left(\frac{dp}{dz}\right)_f = -\left(\frac{dp}{dz}\right)_g \cdot \phi_{CH} \tag{0.45}$$

where the single-phase frictional pressure part should be calculated from the vapour flow instead of the liquid. The two-phase multiplier ϕ_{CH} is

$$\phi_{CH} = x^{1.75}\left[1 + \frac{1}{w_l/w_g} \cdot \frac{1-x}{x} \cdot \frac{\rho_g}{\rho_l}\right]^{2.375} \tag{0.46}$$

where the vapour slip is

$$\frac{w_l}{w_g} = 9.1\left[\frac{1-x}{x}(\mathrm{Re}\,\mathrm{Fr})^{-0.167}\left(\frac{\rho_l}{\rho_g}\right)^{-0.9}\left(\frac{\eta_l}{\eta_g}\right)^{-0.5}\right] \tag{0.47}$$

This model uses the vapour phase as the starting point, thus it should work well for high vapour fractions during annular or misty-annular flow.

Later *Chawla* (1974) had the idea that the model of *Bankoff* (1960) could be used in one area of flow and the model of *Chawla* (1967) in another. The different areas could be determined from the vapour fraction and the ratio of densities between liquid and vapour.

Bankoff (1960) set up the following model:

$$-\left(\frac{dp}{dz}\right)_f = -\left(\frac{dp}{dz}\right)_l \cdot \phi_{Bf}^{7/4} \tag{0.48}$$

where

$$-\left(\frac{dp}{dz}\right)_l = f_l \frac{m^2}{2d_h\rho_l} \tag{0.49}$$

and the two-phase multiplier

$$\phi_{Bf} = \frac{1}{1-x}\left[1-\varepsilon\left(1-\frac{\rho_g}{\rho_l}\right)\right]^{3/7}\left[1+x\left(\frac{\rho_l}{\rho_g}-1\right)\right] \tag{0.50}$$

where

$$\varepsilon = \frac{0.71 + 2.35\left(\rho_g/\rho_l\right)}{1 + (1-x)/x\left(\rho_g/\rho_l\right)} \tag{0.51}$$

3. The experimental facility

An experimental facility has been constructed by *Melin* (1996) to measure heat transfer and pressure drop during horizontal in-tube flow boiling conditions. *Melin* (1996) investigated exclusively smooth tubes where he measured local heat transfer and pressure data.

During this work the whole evaporator part was reassembled using an evaporator tube with a star-shaped insert.

The facility shown in Figure 0-1 consists of four different flow loops. The refrigerant loop, the brine loop, the preheater loop and the condenser loop.

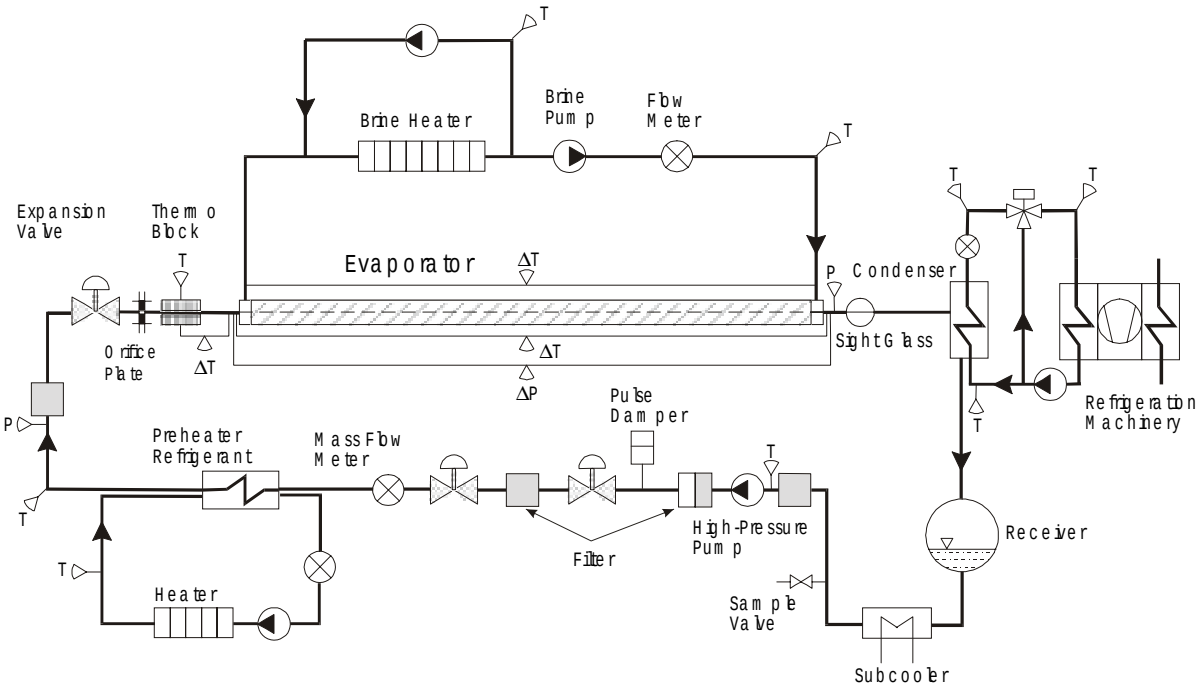

Figure 0-1 Flowchart of the experimental facility

For a Table of instrumentation and its inaccuracies please refer to appendix.

3.1 The refrigerant loop

The refrigerant loop consists of a receiver, a subcooler, a high pressure pump, a corriolis type mass-flow meter, a preheater, an expansion valve, an evaporator and a condenser.

Before the refrigerant reaches the high pressure pump where it can be pressurised up to 25 bar it is subcooled in order to avoid or reduce the risk of cavitation. Leaving the pump, a pulse-damper and filters ensure that the following flow measurement is not disturbed by any means.

In the preheater the refrigerant is heated up to nearly saturation temperature and just before the expansion valve the refrigerant's state can be captured by pressure and temperature measurement. Another pressure and temperature measurement after the expansion valve ensures the determination of vapour fraction at the inlet of the evaporator. Eventually the evaporator (for detailed description of the evaporator see further down) is followed by a condenser where all vapour is condensed before it is collected in the receiver.

3.2 The brine loop

The brine is heated electrically and the flow through the heater is increased by using a second loop only to get quicker response from a change in heat input.

The brine's flow is measured with an inductive flow meter and a Pt 100 resistance thermometer measures it's absolute temperature just before entering the evaporator. Once the brine has reached the evaporator it flows through an annulus in counter flow to the refrigerant along the inner tube.

3.3 The preheater loop

The liquid in the preheater loop is warmed by an electrically driven heater. The flow is measured using an inductive flow meter, the temperature difference over the preheater as well as the absolute temperature is measured.

The size of the heat exchanger between the working fluid and the preheater fluid is large, making the temperature difference between the two fluids small. This allows strict control of the refrigerant temperature, since the preheater can be run close to saturation without running the risk of superheating the working fluid.

3.4 The condenser loop

The liquid in the condenser loop (55% ethylene glycol by weight in water) is cooled by an water-cooled refrigeration machinery. The cooled liquid is stored in a 1.5 m^3 tank where the temperature is kept constant. The liquid is pumped through a three-way valve which splits it into two streams of which one cools the condenser. The flow of this stream is measured by using an inductive flow meter. The temperature difference over the condenser is measured.

3.5 The evaporator

As seen in Figure 0-2 the experimental evaporator consists amongst other things of a four meter horizontal ten channel tube (for dimensions refer to the appendix). The internal channels are produced by a star-shaped insert with radially-diverging longitudinal fins. The shell is made of copper, which is resistant to corrosion by brines and is inert to refrigerants. The insert is aluminium, which has a low density, high thermal conductivity and inertness to refrigerants.

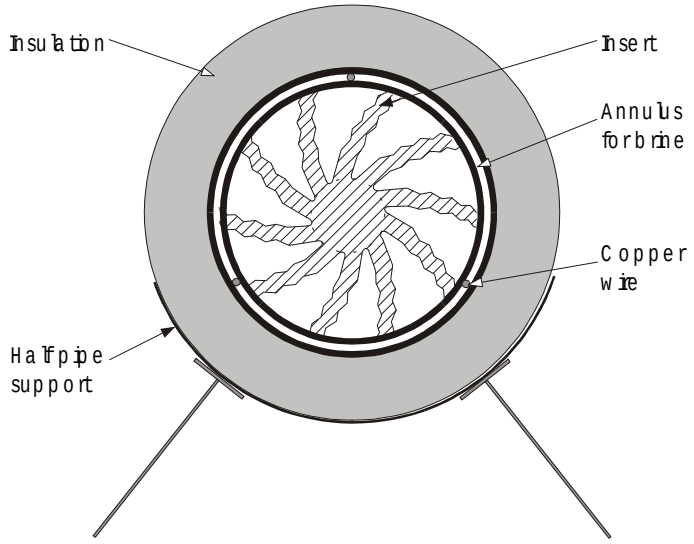

Figure 0-2 Evaporator cross-section (not to scale)

Brine is employed as the shell-side heating medium. It is pumped through an annulus in concurrent flow with the refrigerant on the tube side. This annulus was created by a second, larger, tube surrounding the actual evaporator tube and using 1.5 mm wires as distance holders between inner and outer tube.

The thickness of the annulus has been kept small (1.5 mm) so that the heat transfer coefficient on the outside will be large enough to make the total heat transfer more dependent on the

inside heat transfer than on the outside. This small hydraulic diameter resulted in a large pressure drop, which made it necessary to change the brine pump.

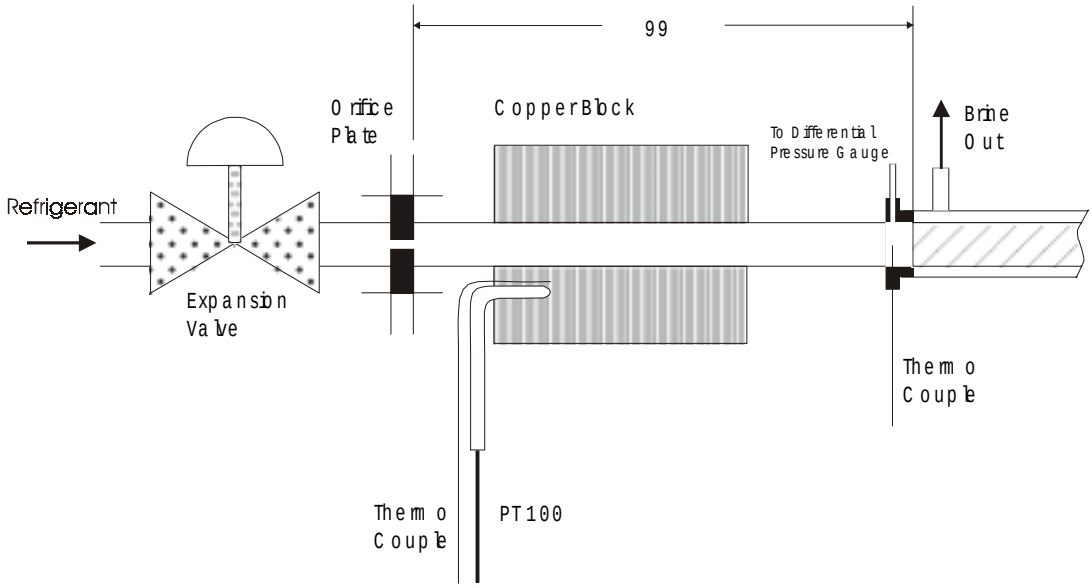

Figure 0-3 Inlet arrangement of the test section

The inlet arrangement, shown in Figure 0-3, was chosen to resemble those conditions of an evaporator tube found in the large scale application. Therefore the refrigerant is flashed through an expansion valve and distributed to the evaporator via an orifice plate.

The copper block was installed as a reference point for temperature measurement. Here the absolute temperature is measured, making it possible to determine the evaporator inlet and outlet temperature using thermocouples.

Eventually it should be mentioned that the evaporator as well as the whole facility was thoroughly insulated.

3.6 Measurements in test section

The evaporator is hydraulically and thermally a single unit meaning that pressure and temperature are measured only at evaporator inlet and outlet. The absolute temperatures have all been measured using Pt 100 resistance thermometers, and the temperature differences using type T (copper-constantan) sheathed thermocouples. The diameter of the thermocouples is 0.5 mm.

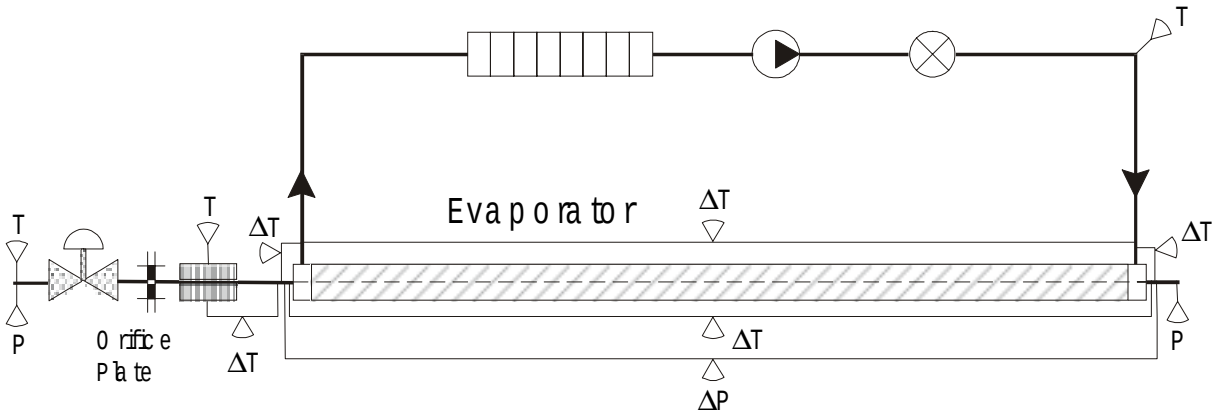

Figure 0-4 Measurements at the test section

The arrangement of measurements are shown in Figure 0-4. Thermocouples are installed between copper block and evaporator inlet, evaporator in- and outlet, brine in- and outlet, brine inlet and evaporator outlet and brine outlet and evaporator inlet. Absolute temperatures were measured before the expansion valve, in the copper block and at brine inlet.

The pressure drop in the evaporator was measured using a differential pressure transducer and measuring the absolute pressure at evaporator outlet (condenser pressure) the inlet pressure was also calculable. Absolute pressure was also measured before the expansion valve.

3.7 Plant control

The experimental plant is controlled by 6 external regulators. The properties controlled by the regulators are:

- *Refrigerant flow*. The mass-flow meter outputs an analog signal to a regulator that controls the frequency of the current to the refrigerant high-pressure pump.
- *Refrigerant temperature after the preheater*. The temperature of the refrigerant before the expansion valve is controlled by the heat input from the electric heater. The heater is controlled, via a thyristor, by a regulator.
- *Refrigerant pressure between high-pressure pump and expansion valve*. The pressure is measured by an absolute pressure transducer and an analog signal is sent to the regulator, which then controls the pressure via the expansion valve.
- *Condenser pressure*. The condenser pressure is regulated via a by-pass valve controlling the flow of liquid through the condenser. The temperature of the glycol-water mixture running through the condenser is kept constant.

- *Brine flow*. On the brine side the flow is regulated by frequency control of the brine pump. The flow is measured by an inductive flow meter.
- *Brine temperature*. Brine temperature , measured in the loop around the heater, is kept constant by an regulator controlling the electric heater via a thyristor.

3.8 Data acquisition and system control

All pumps, heaters, magnetic valves and regulators in the system are controlled by a personal computer. The pumps, heaters and magnetic valves are controlled via an I/O-card that operates a relay box. Through this I/O-card all alarms and indications for the pumps and heaters are sent to the computer. The coriolis-type mass-flow meter is connected directly to the PC by a RS-485 interface. All the thermocouples, Pt 100 resistant thermometers and V/A signals are connected to a data logger and read by a multimeter.

The PC gives the setpoint to the regulators and reads the output and the current value. The inductive flow meters on the preheater and condenser loops give 5760 pulses for each litre of fluid. These pulses are counted by an event counter with a maximum value of 10 million. This event counter is also connected to the Computer through the RS-485 interface.

The control program was originally set up by *Melin* (1996) and adjusted to the new arrangement of measurements during this work. As part of the calibration process, new equations were introduced to convert the current and voltage signals into the respective output parameter like temperature, pressure or flow.

When measuring and saving data during the runs they are read three times and put into an output file. This enables to compare data of the same state and identify accidental disturbances.

3.9 Calibration of instruments

All flow meters have been calibrated by an authorised measuring centre. The multimeter used for the thermocouples, Pt 100 resistant thermometers and the ampere signals has been calibrated by the Swedish National Testing Institute. They also calibrated the quartz thermometer later used for calibrating the thermocouples and Pt 100 resistance thermometers. The quartz thermometer’s accuracy is stated to be +/- 0.01 °C.

The pressure gauges were calibrated on-site by using a portable calibration unit.

4. Experimental procedure

Experiments were started with the tube (tube 1) which claimed to show better performance in large scale applications. The measurements on this tube were used as reference for the comparison.

When those measurements were completed, the second tube (tube 2) was prepared, meaning equipped with an annulus for brine heating using exactly the same design as for tube 1. After connecting tube 2 to the test section, different comparison runs were conducted.

For all experiments pure HCFC22 as refrigerant was used.

4.1 Experiments - tube 1

4.1.1 Preliminaries

Preliminary tests were conducted to ensure that the working fluid was not contaminated with oil. This was done by observation of fluid coming out of the evaporator using the sight glass. Starting in the two-phase region, the brine temperature was slowly increased until the output temperature started to rise and therefore complete evaporation of refrigerant had happened. If then oil was observed the refrigerant was replaced. This procedure was repeated until all oil was ‘washed out’. When no oil was detected anymore the actual measurements were started.

4.1.2 Reference measurements

The experimental conditions for measurements with tube 1 are listed in Table Table 0-1.

Table 0-2 Range of experimental conditions

PROPERTY		RANGE
Temperature before expansion valve	(°C)	24
Pressure before expansion valve	(bar)	11
Inlet pressure	(bar)	4.7 - 5.2 (depending on refrigerant flow)
Inlet temperature	(°C)	1.0 - (-2.0), equilibrium (see inlet pressure)
Inlet vapour fraction	(%)	13 -14
Outlet pressure	(bar)	≈ 4.6
Outlet superheat temperature	(°C)	8.0 - 10.5
Refrigerant flow	**(g/s)**	**14 - 34**
Brine inlet temperature	**(°C)**	**8, 10, 12**
Brine flow	(g/s)	260

Different superheat regions were investigated using the different brine inlet temperatures. **Sabroe Refrigeration AB** was especially interested in the 8 °C superheat region, as this is what they usually run in their large scale applications. The range of brine inlet temperatures was given by **Sabroe Refrigeration AB** as well.

Since at 8 °C superheat the refrigerant flow was relatively large, higher superheat regions were investigated as well. It was of interest to test the tube's behaviour for lower flows at the same brine temperature, which of course increased the superheat temperature. Test conditions were

Superheat: 8,0 - 8,5 °C → Brine In: 8 °C, 10 °C, 12 °C

Superheat: 8,5 - 9,0 °C → Brine In: 8 °C, 10 °C, 12 °C

Superheat: 9,5 - 10,5 °C → Brine In: 8 °C, 10 °C, 12 °C

When all desired conditions were set, the facility was run for 3 hours to ensure that steady state was reached.

4.2 Experiments - tube 2

Measurements with tube 2 were performed in two different ways making a comparison possible. First all conditions were held the same as for the runs with tube 1, which mainly meant keeping the refrigerant flow equal. Here the resulting superheat was investigated. If the deviation of superheat temperature was larger than +/- 0.4 °C the refrigerant flow was changed such that the same superheat was achieved as in experiments with tube 1. A comparison of refrigerant flows was carried out in this case. Below the two series of experiments are summarised:

A. **Same refrigerant flow** as measurements with tube 1. Investigation of **superheat**
B. **Same superheat** as measurements with tube 1. Investigation of **refrigerant flow**

4.3 Detection of superheat starting point

To not only cover test conditions where superheat occurs but also conditions of incomplete evaporation, measurements around the starting point of superheat were taken.

The brine inlet temperature was held constant at 10 °C and the refrigerant flow was varied stepwise between 38.4 g/s (two-phase flow was visible) and 29.4 g/s (no liquid was visible). All other parameter were set as stated in Table Table 0-1.

Another reason for the investigation of the superheat starting point was the knowledge of an error in heat balance that occurred in earlier experiments by *Melin* (1996). The calculation of the maximum vapour fraction before complete evaporation can be an additional indicator for sources of errors in heat balance.

5. Measurement results

As an example for the output data from the measurements, Table Table 0-1 shows a complete set of reference and comparison data.

Table 0-1 Example of measurement data

	Tube		Tube 1	Tube 2	Tube 2
			Reference	Same Refrigerant flow	Same Superheat
	This are the measurement results from:		Time 20:36:12 Date 01-20-1998	Time 13:50:30 Date 01-27-1998	Time 16:01:29 Date 01-27-1998
		Unit			
1	Freon flow average value for the entire reading	kg/s	0,03404	0,03412	0,03508
2	Temperature before expansion valve	°C	23,864	23,857	23,846
3	Pressure before expansion valve	bar	11,093	11,054	11,053
4	Temperature refrigerant in	°C	1,035	1,052	1,182
5	Pressure refrigerant in	bar	5,151	5,151	5,176
6	Enthalpy refrigerant in	J/kg	228 860,000	228 852,000	228 838,000
7	Vapour fraction	%	13,550	13,546	13,461
8	Temperature diff. refrigerant in and out	°C	5,399	6,039	5,298
9	Pressure diff. refrigerant in and out	bar	0,508	0,511	0,531
10	Enthalpy difference	J/kg	181 458,000	181 945,000	181 511,000
11	Temperature refrigerant out	°C	6,434	7,091	6,480
12	Pressure at evaporarator outlet	bar	4,643	4,641	4,644
13	Temperature at dew point	°C	-2,14	-2,15	-2,13
14	Superheat temperature	°C	8,574	9,241	8,610
15	Enthalpy refrigerant out	kJ/kg	410 318,000	410 797,000	410 349,000
16	Temperature brine in	°C	12,070	12,058	12,093
17	Temperature difference brine in and out	°C	5,224	5,258	5,372
18	Temperature brine out	°C	6,846	6,801	6,722
19	Brine flow	g/s	260,654	260,421	260,394
20	Brine velocity	m/s	2,700	2,697	2,697
21	**Re Number**		**6 197,101**	**6 191,555**	**6 190,927**
22	**Transferred heat from brine side**	**W**	**5 732,966**	**5 764,380**	**5 888,882**
23	**Transferred heat on refrigerant side**	**W**	**6 176,781**	**6 207,070**	**6 367,326**
24	Deviation	%	7,185	7,132	7,514
25	Transferred heat from brine side / area$_{(outer\ tube)}$	W/m^2	25 255,355	25 393,743	25 942,210
26	Mean Δ T_{ln} (using dew point temperature)	°C	11,399	11,378	11,326
27	**Overall htc U_m (no concideration of superheat)**	**W/(m^{2}K)**	**2 211,421**	**2 227,749**	**2 286,265**
28	**Overall htc U_m (numerical determination)**	**W/(m^{2}K)**	**2 640,200**	**2 651,200**	**2 745,540**
29	**Outer heat transfer coefficient α_o**	**W/(m^{2}K)**	**9117,159**	**9108,811**	**9113,931**
30	**Inner heat transfer coefficient α_I**	**W/(m^{2}K)**	**9588,124**	**9684,676**	**10022,421**

For a collection of all data tables, please see the appendix.

5.1 Calculations

The following explanations to Table Table 0-1 refer to the numbers in the first column .

1, 2, 3, 8, 9, 12, 16, 17, 19 were measured directly.

4 Absolute temperature thermoblock minus temperature difference thermoblock and inlet

5 Absolute pressure at evaporator outlet plus pressure difference (**9**)

6 A computer package for thermophysical data was used to determine the inlet and outlet enthalpies, the inlet vapour fraction and the dew point temperature. The equation of state for HCFC22 used in the program was developed by *Kamei and Beyerlein* (1991). The enthalpy was determined using **2** and **3** and under the assumption of isenthalpic expansion through the expansion valve.

7 **5** and **6** into the computer package (see **6**)

10 **15** minus **6**

11 **4** plus **8**

13 Calculated from **12**

14 **11** minus **13**

15 Computer package with **11** and **12** (see **6**)

18 **16** minus **17**

20
$$w_{Brine} = \frac{\dot{M}_{Brine}}{A \cdot \rho} \tag{0.52}$$

21
$$\mathrm{Re} = \frac{w \cdot d_h}{\nu} \tag{0.53}$$

22
$$\dot{Q}_{Brine} = c_p \cdot \dot{M}_{Brine} \cdot \Delta T \tag{0.54}$$

23
$$\dot{Q}_{\mathrm{Ref}} = \Delta h \cdot \dot{M}_{\mathrm{Ref}} \tag{0.55}$$

24 Deviation between **22** and **23**

26
$$\Delta T_{\ln} = \frac{(\mathbf{16} - \mathbf{13}) - (\mathbf{18} - \mathbf{4})}{\ln \frac{(\mathbf{16} - \mathbf{13})}{(\mathbf{18} - \mathbf{4})}} \tag{0.56}$$

27

$$U_m = \frac{\dot{Q}_{Brine}}{A_{Outer\ tube} \cdot \Delta T_{\ln}} \tag{0.57}$$

Note that here there is no consideration of superheat!

28 This overall heat transfer coefficient was achieved in an iterative way using a computer program. The measured data was given as input and the respective U-value was then calculated with the application of the following mean temperature difference

$$\Delta T_{mean} = \frac{1}{\left(\sum_{h_{in}}^{h_{out}} \frac{\Delta h_{step}}{\Delta h_{total} \Delta T_{step}} \right)} \tag{0.58}$$

To take the significant decrease of the U-value in the superheat region into account, the mean temperature difference was here corrected by a factor 3.5. The factor 3.5 was determined during earlier simulations by comparing calculated local U-values in the two-phase region and in the single-phase vapour region.

$$\left(\Delta T_{mean}\right)_{SH} = \left(\Delta T_{mean}\right)_{calc} \cdot 3.5. \tag{0.59}$$

29 See equation (2.42)

30 See equation (2.5) using U from **27**

5.2 Comparison of superheat.

A. Brine Inlet Temperature 8 °C.

This is the lowest investigated refrigerant flow region with 0.020 kg/s to 0.024 kg/s resulting in superheat of 9.7°C to 8.0°C respectively. The results are shown in Figure 0-1. Tube2's performance was in all cases worse than tube1's performance varying between **-10% and -18 %**

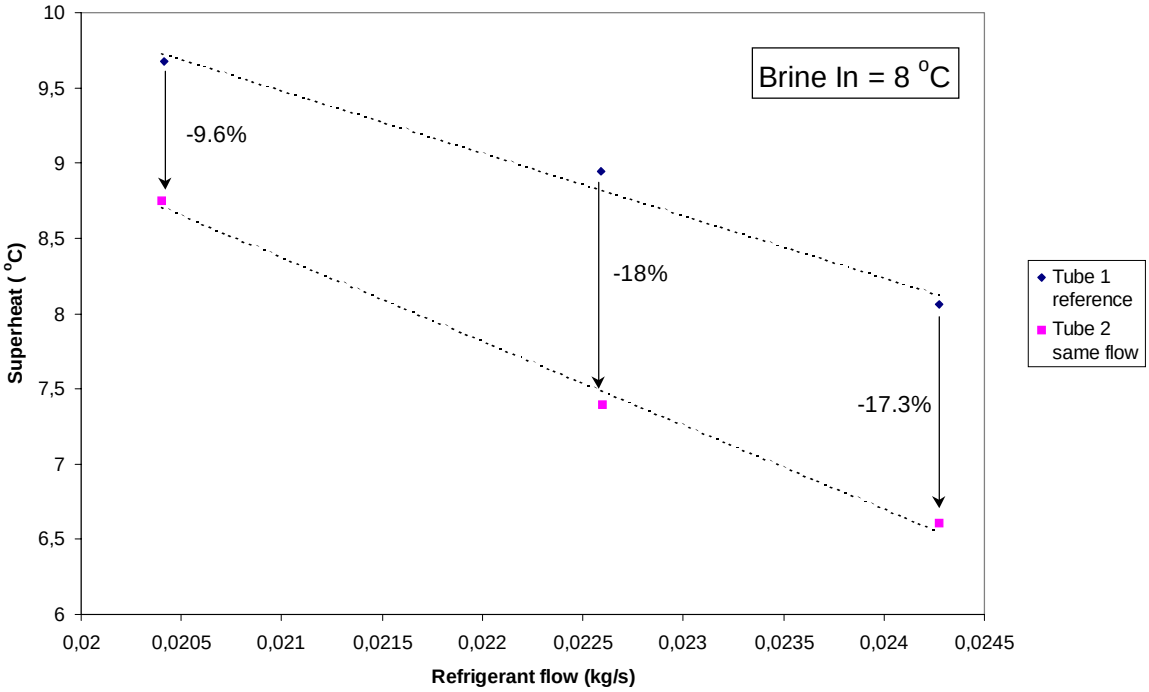

Figure 0-1 Superheat temperature versus refrigerant flow at brine inlet temperature 8°C

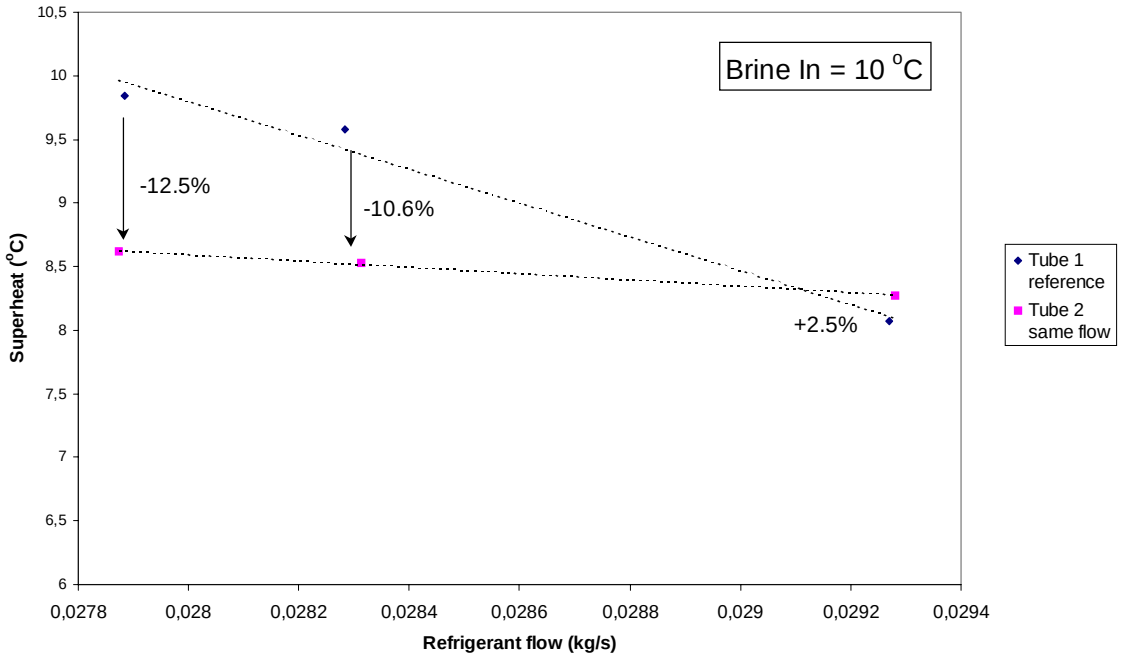

Figure 0-2 Superheat temperature versus refrigerant flow at brine inlet temperature 10°C

B. Brine Inlet Temperature 10 °C.

Representing the mean refrigerant flow region of the experiments with a flow between 0.028 kg/s and 0.029 kg/s and resulting superheat between 9.8°C and 8.0°C, tube 2's per-

formance was worse at lower flow (**-12.5% and -10.6%**) but improved at higher flows (**+2.5%**). The results are shown in Figure 0-2.

C. Brine Inlet Temperature 12 °C.

Here the highest flow region is represented. The refrigerant flow was varied between 0.033 kg/s and 0.035 kg/s to achieve superheat of 10.4°C to 8.3°C. The performance of tube 2 was in all cases better and improved at higher flows **(+4% to +22%)** which is shown in Figure 0-3**.**

The two data points of tube 2 in the high refrigerant flow region have been rechecked by repeating those measurements. The results were the same as the first time.

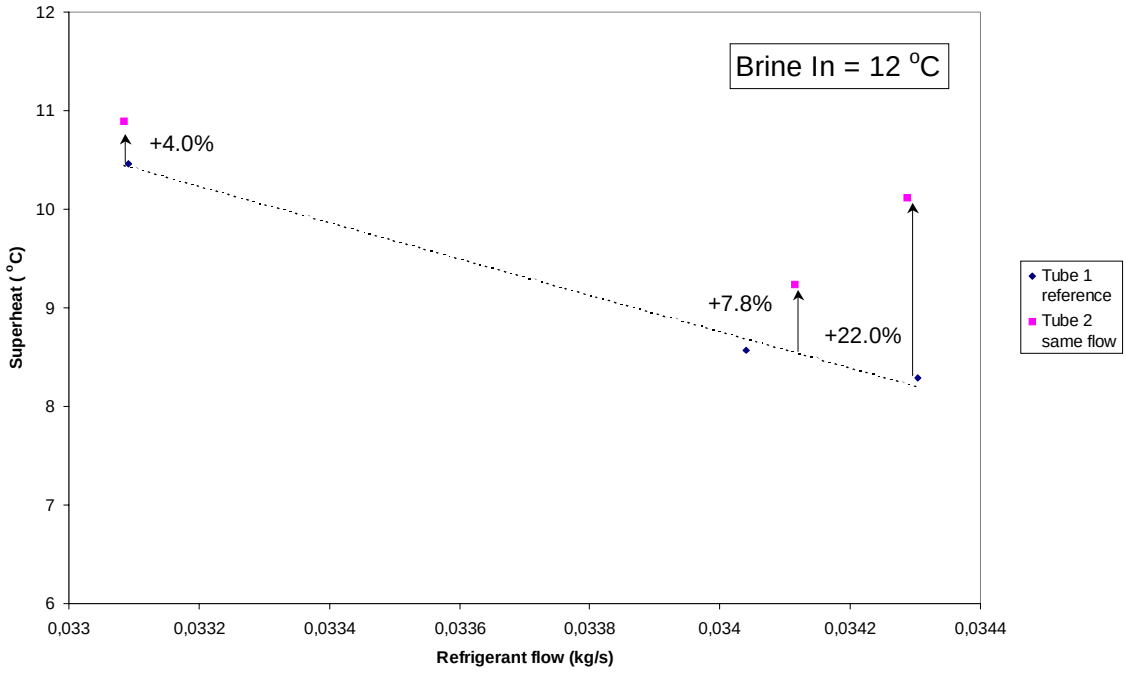

Figure 0-3 Superheat temperature versus refrigerant flow at brine inlet temperature 12°C

5.3 Comparison of refrigerant flow

The second series of results shows how the refrigerant flow had to be changed in order to reach the same superheat as in experiments with tube 1.

A. Brine Inlet Temperature 8 °C.

To achieve the same superheat, the refrigerant flow in tube 2 had to be decreased in all

cases. Especially at high superheat where the flow went down to 0.014 kg/s which is **29%** lower as in tube 1. See Figure 0-4 for results.

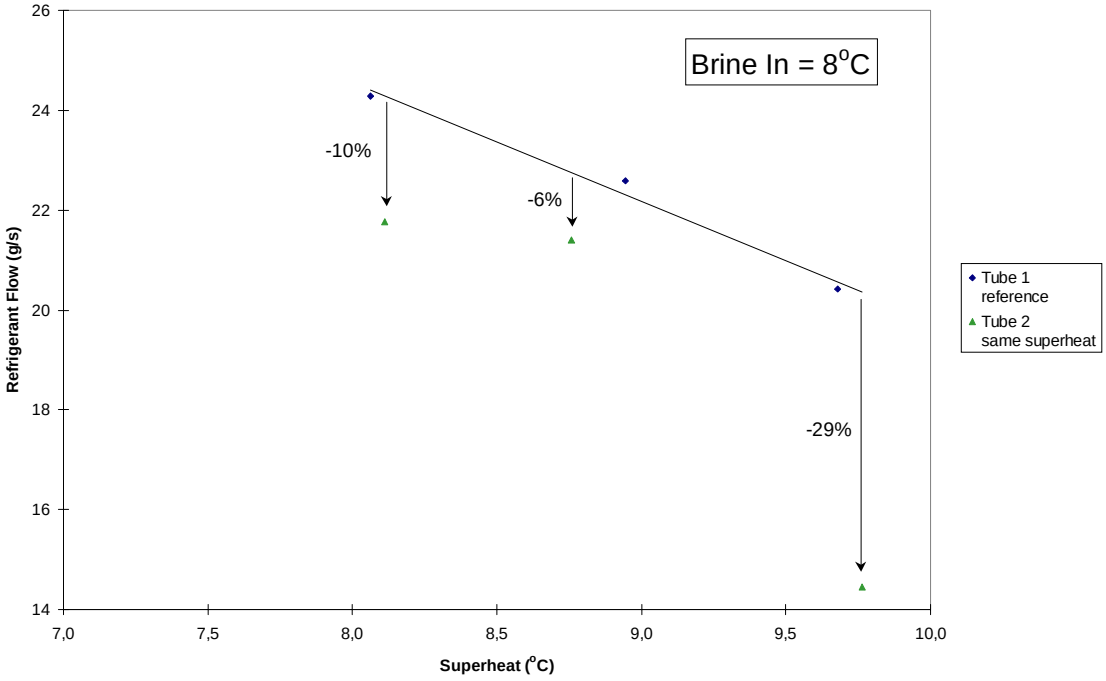

Figure 0-4 Refrigerant flow versus superheat temperature at brine inlet temperature 8°C

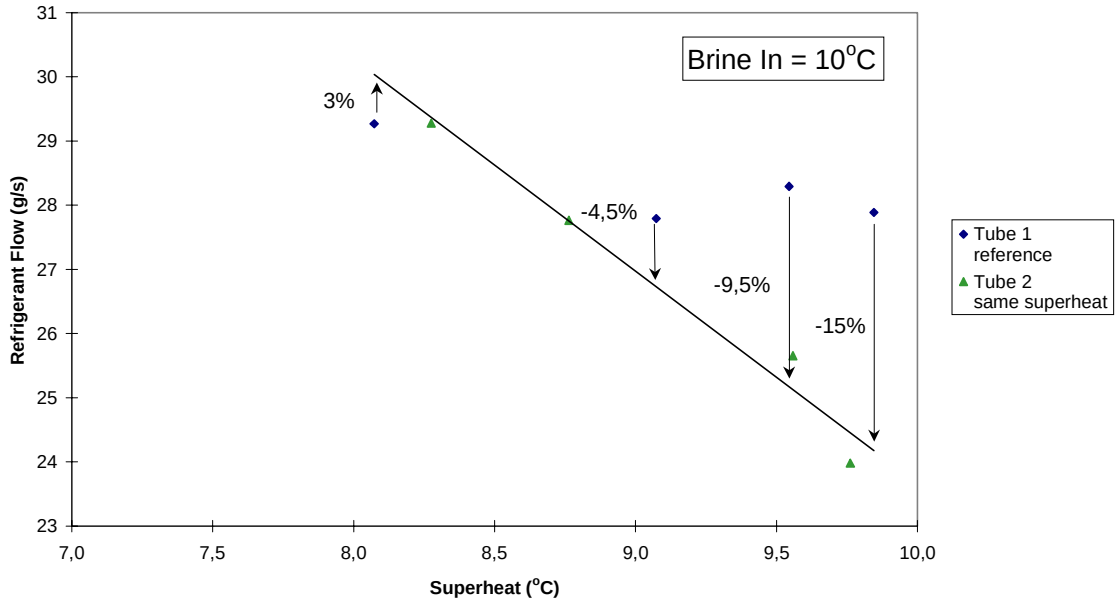

Figure 0-5 Refrigerant flow versus superheat temperature at brine inlet temperature 10°C

B. Brine Inlet Temperature 10 °C.

In Figure 0-5 the decreasing performance of tube 2 at higher superheat is seen. From **+3%** at 8°C superheat to **-15%** at 9,8°C superheat.

C. Brine Inlet Temperature 12 °C.

As is shown in Figure 0-6, in all cases the refrigerant flow for the same superheat is higher. However, this better performance decreased at higher superheat (from **+7%** at 8.3°C superheat to **+0,7%** at 10.4°C superheat).

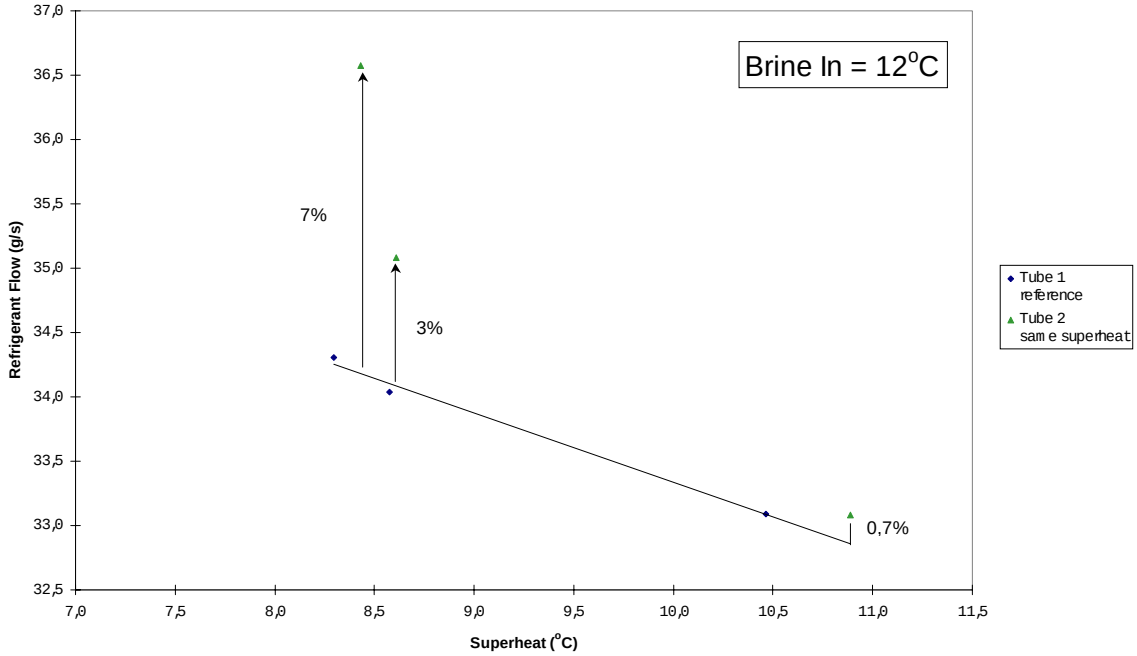

Figure 0-6 Refrigerant flow versus superheat temperature at brine inlet temperature 12°C

The different methods of comparison are of course related to each other and can be shown in the same diagram which is also a way of verifying the consistency of the results.

In Figure 0-7 it is emphasised how the data points are related to each other. Starting from the reference data point of tube 1, in vertical direction the first comparison series is represented where the same flow was used. In horizontal direction one can see the second measurement series where the same superheat was adjusted and the refrigerant flow investigated. The circled points were the object of just one comparison run due to almost identical superheat at the same refrigerant flow.

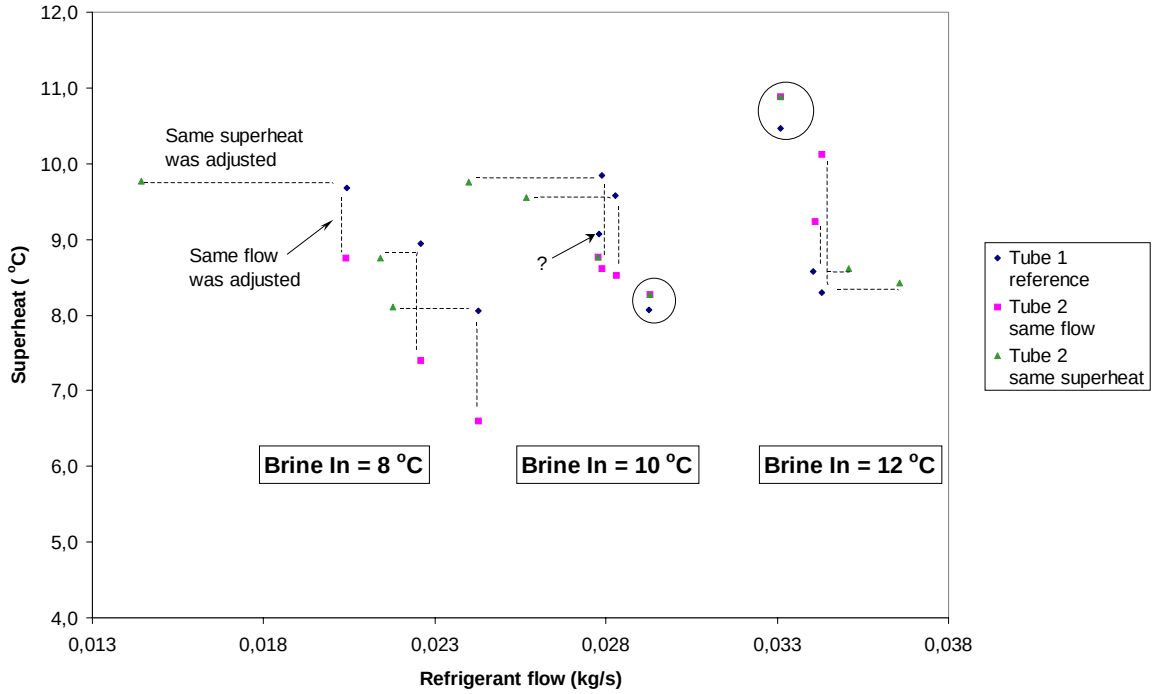

Figure 0-7 Summary of all measurements

5.4 Superheat starting point

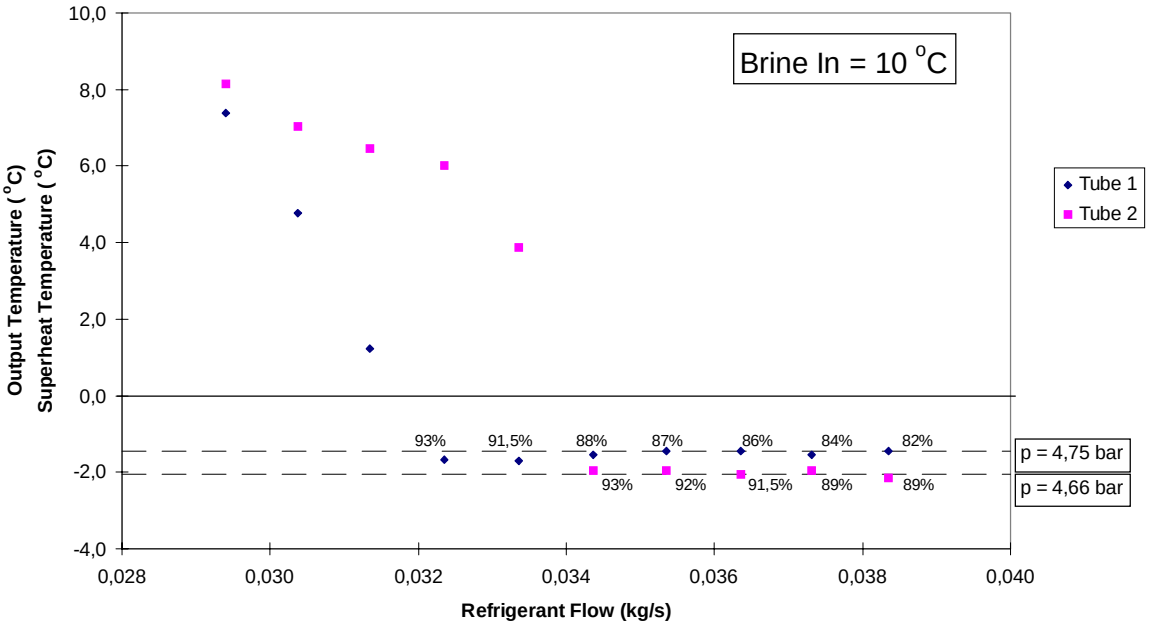

Figure 0-8 Detection of superheat starting point at constant brine inlet temperature of 10 °C

Figure 0-8 shows the outlet conditions of both tubes at varying refrigerant flows at a constant brine inlet temperature of 10 °C. During two-phase flow at the outlet, the vapour fraction in tube 2 was higher than in tube 1 resulting in a complete evaporation at a higher flow. This is to some extend due to the different condenser pressures at measurements with tube 1 and tube 2.

In the superheat region tube 2 showed always higher temperatures which, however, continuously decreased to lower flows.

It has to be mentioned that the highest calculated vapour fraction before complete evaporation is 93% (see chapter 6 for discussion).

6. Discussion

6.1 Possible causes for difference in performance

The fact that the results do not show a general superior behaviour for one of the compared tubes suggests that the test conditions actually determine the performance of the tubes. In order to explain this situation, a closer examination of the main influencing factors and their relation to mass and heat flux must be performed. These factors are:

- Insert-shell connection
- Distribution between the different channels
- Surface structure of the insert

6.1.1 Insert-shell connection

The most obvious thing to consider when attempting to explain the difference in performance, is the insert-shell connection. The whole enhancement in heat transfer due to area enlargement is dependent on unrestricted heat conduction from shell to insert. The lower performance of tube 2 (at lower refrigerant flow and 8°C brine inlet temperature) could be explained by imperfect heat conduction between the copper shell and the aluminium insert. The internal area enhancement is then to a great extent wasted.

A physical survey of the two tubes showed a significant difference in insert connection to the shell. Tube 2's connection is much looser and the insert could easily be removed from the shell which was impossible with tube 1. Gaps between insert and shell of tube 2 can be observed and at the insert ends there is hardly any contact at all. This situation may well worsen at low temperature evaporation, since the coefficient of linear expansion of aluminium is higher than that of copper. A reduced contact pressure then occurs.

However, a higher brine temperature and therefore a higher driving force should then result in an even (stronger) manifestation of the above. The better performance of tube 2 in this test region thus seems to contradict this hypothesis.
A possible way to resolve this contradiction could be a higher degree of refrigerant mixing due to an exchange between the channels. In an earlier investigation of tubes with star-shaped inserts by *Kubanek and Miletti* (1979) it is mentioned that the heat transfer enhancements decreased with increasing mass velocity. They suggested that this might be due to the fact that the radial splines separate the tube into ten compartments, and thus limit the degree of mixing which would normally occur with increased flow rates were the tube is not compartmentalised. If there is considerable fluid exchange between the channels, heat transfer might even be enhanced making tube 2 more efficient than tube 1.

Since there is a difference in manufacturing resulting in an obvious difference in insert-shell connection , it is therefore very likely that this plays a major role when explaining the difference in performance.

6.1.2 Distribution between the different channels

A further influencing factor is the distribution between the different channels. If the insert ends are not properly treated and the entrance areas of the channels are different, the flow distribution varies between them. In this case some channels are used in a sub-optimal way and a loss in effective evaporator area results. Different distribution might also occur during the process of flashing the refrigerant into the evaporator tube.

The channel edges of tube 2 are visibly burred, possibly resulting in the above mentioned loss in effective evaporator area and a worse performance than tube 1.

Different mass flows in the ten channels would result in pressure differences between the channels, increasing with greater velocities. Tube 2 might be able to even out the different channel flows by exchanging fluid through the insert-shell gaps, especially at higher flows where tube 2 indeed showed improved performance.

However, the overall pressure drop at same refrigerant flows was almost identical for both tubes, suggesting that the differences in flow distribution between the different channels are insignificant.

Furthermore it is difficult to evaluate the influence of the flow distribution because the flow patterns at the outlet of the orifice plate at changing flows are completely unknown.

6.1.3 Surface structure of the insert

The microscopic surface structure of the insert has major influence on nucleate boiling. The generation of vapour in crevices and cavities which act as so called nucleation sites could be another way of explaining the different behaviours of the two tubes.

It might be the case that tube 1's insert provides more nucleation sites than tube 2's and therefore the nucleate boiling contribution in tube 1 is higher at lower mass flows.

As seen in Figure 2-4 the nucleate boiling is suppressed at higher flows where forced convective evaporation dominates. Here tube 2 could gain compared to tube 1 for the afore-given reasons.

An earlier investigation of a ten channel tube by *D'Yachkov* (1978) showed that in a mass flow region which was in the same range as in this project, high heat fluxes manifested themselves at low values of vapour fractions. Here the region of nucleate boiling became explicit. Of course it is always difficult to compare different investigations, because they might have been conducted in very different conditions.

The vapour fraction was already between 13% and 14% at the evaporator inlet and the heat flux was by far not as high as in the investigation quoted above. Therefore it should be possible to assume that the microscopic surface structure is negligible when explaining the measurement results.

6.1.4 Summary

All of the above discussed factors may well contribute to the observed difference in the performance of the two tubes. More detailed investigations are necessary to identify which factors occur and to what extent. Such an investigation cannot be performed with the existing experimental facility, which only records data at the inlet and outlet of the evaporator.

A sectional measurement of wall and liquid temperatures at different points of circumference could give much better information about local heat transfer coefficients and channel flow distribution. However, building such a testing facility is a complicated and time consuming task, well beyond the scope of this study.

6.2 Practical significance

Sabroe Refrigeration AB detected a significantly worse performance of tube 2 in their large scale tests. Since in this project systematic worse performance could not be observed, their large scale test conditions should be discussed.

The large scale test conditions were the following: 9.5 g/s refrigerant flow, 15% inlet vapour fraction, 9.2 °C brine temperature and 9 °C superheat. Brine system: counter flow with baffles.

The test conditions are different since the refrigerant flow is much lower than most of the investigated flows of this work. Therefore just the lower tested flow region allows a comparison with the large scale tests done by **Sabroe Refrigeration AB**. Here their results could be confirmed.

However, it is important to point out that in those conditions where **Sabroe Refrigeration AB** identified differences between the tubes, the fluid is distributed among many of tubes where some receive more and some less than the average flow, and thus the overall heat transfer of the evaporator will decrease.

6.3 Error in heat balance

As seen in Table 5-1 there is a 7 % deviation between transferred heat on brine and refrigerant side. This error manifests itself as well when comparing outlet vapour fraction in Figure 5-8 where the maximum calculated vapour fraction before complete evaporation is 93%.

For the discussion of possible causes for this error, it is helpful to show the equation for the outlet vapour fraction x^*:

$$x^* = \frac{1}{\Delta h_v}\left(\frac{\dot{Q}_{Brine}}{\dot{m}} + h_{in} - h_l\right) \qquad (0.1)$$

Since the pressure transducers, the thermocouples and the Pt 100s have been calibrated carefully and their inaccuracy is very low (see Table of instrumentation in appendix), the contribution of the enthalpies in equation ((0.6)) to the error is negligible.

The transferred heat through the insulation has been calculated to less than 1.5 W/K temperature difference to the environment. This is about 0.3% of the transferred heat from the brine side.

Finally there are just the brine and the refrigerant flow meters which could be the reason for the error in heat balance. Both flow meters were calibrated by an authorised measuring centre five years ago. It is unknown how the past five years and a reconstruction of the whole facility could have affected their accuracy. Furthermore the flow meters were both calibrated with water and the flow meter for the refrigerant flow went through some modifications to make it explosion proof. Thus it is likely that the refrigerant flow meter is the main source of error. For the future it is recommended to recalibrate the flow meters on a regular basis.

7. Numerical comparison

Since there is a lack of data like that measured during this project, it can be a valuable contribution for validation of the simulation program used in the Department of Heat and Power Technology. This chapter aims to compare measured and calculated data.

7.1 Simulation program

At the Department of Heat and Power Technology, a comprehensive computer program has been developed where whole refrigeration systems as well as single components can be simu-

lated. For the calculation of heat transfer and pressure drop, numerical integration along the evaporator tube is used. Thermodynamic and transport properties are taken from a property calculation package which is connected to the main simulation program.

Models for the calculation of heat transfer are the ones from *Pierre* (1969) - equation (2.7), *Shah* (1976) - equation (2.9), *Klimenko* (1988) - equation (2.16) and *Melin* (1996) - equation (2.25). *Melin's* originally developed correlation does not cover vapour fraction above 95%. However, this correlation as well as the ones from *Shah and* Klimenko was modified by *Gabrielii* (1997) according to *Dittus and Boelter* (1985), to cover the heat transfer coefficient at high vapour qualities. For the single-phase vapour region a separate heat transfer correlation by *ESDU* (1967) is used.

Pressure drop was compared to the correlation from *Pierre* (1957) and the one from *Chawla* (1967) and *Bankoff* (1990).

To make the correlations above applicable, the specific geometrical parameters as hydraulic diameter and evaporation area of the tubes with inserts were added.

Input:

- Evaporator configuration.
- Refrigerant and brine identification numbers and equations of state.
- On refrigerant side: flow before evaporator, pressure and temperature after evaporator.
- On brine side: flow and temperature before evaporator, pressure after evaporator, pressure drop.
- Outer heat transfer coefficient.

Output:

- On refrigerant side: pressure and vapour fraction before evaporator.
- On brine side: temperature after evaporator.
- Deviation between calculated and measured overall heat transfer coefficient given as the fraction U_{meas}/U_{calc}. A factor below 1 means an overestimation, a factor over 1 an underestimation of heat transfer.

7.2 Results

7.2.1 Heat transfer - tube comparison

All four heat transfer correlations display similar behaviour when comparing the two tubes. As an example *Shah's* (1976) correlation is compared with experimental data in Figure 0-1.

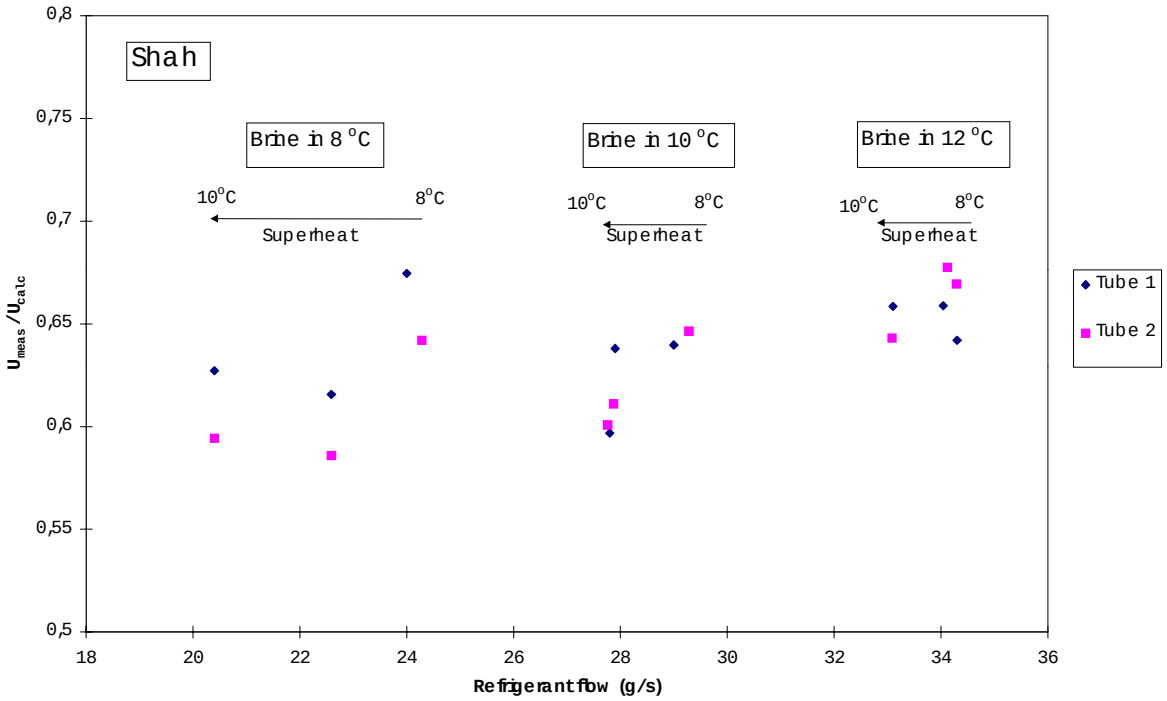

Figure 0-1 Comparison of the two tubes by using Shah's correlation

At 8 °C brine inlet temperature in the low refrigerant flow region, the deviations for tube 2 are in all cases larger than for tube 1. This situation changes with higher refrigerant flows. At 10°C brine inlet temperature the deviation for tube 2 is in one case larger, otherwise the same as for tube 1 and at a brine temperature of 12 °C it is mostly smaller than for tube 1.

Since for both tubes the calculated values are the same, a difference in deviation factor is just a manifestation of the different measured values and a higher deviation for tube 2 means a worse performance whereas a lower deviation for tube 2 indicates a better performance.

7.2.2 Heat transfer - correlation comparison

A comparison of the different correlations for tube 1 is seen in Figure 0-2. All correlations overestimate the inner heat transfer coefficient resulting in a deviation factor from 0.7 to 0.45. Within this deviation range, *Shah* (1976) performs best followed by *Melin* (1996), *Klimenko* (1988) and *Pierre* (1969).

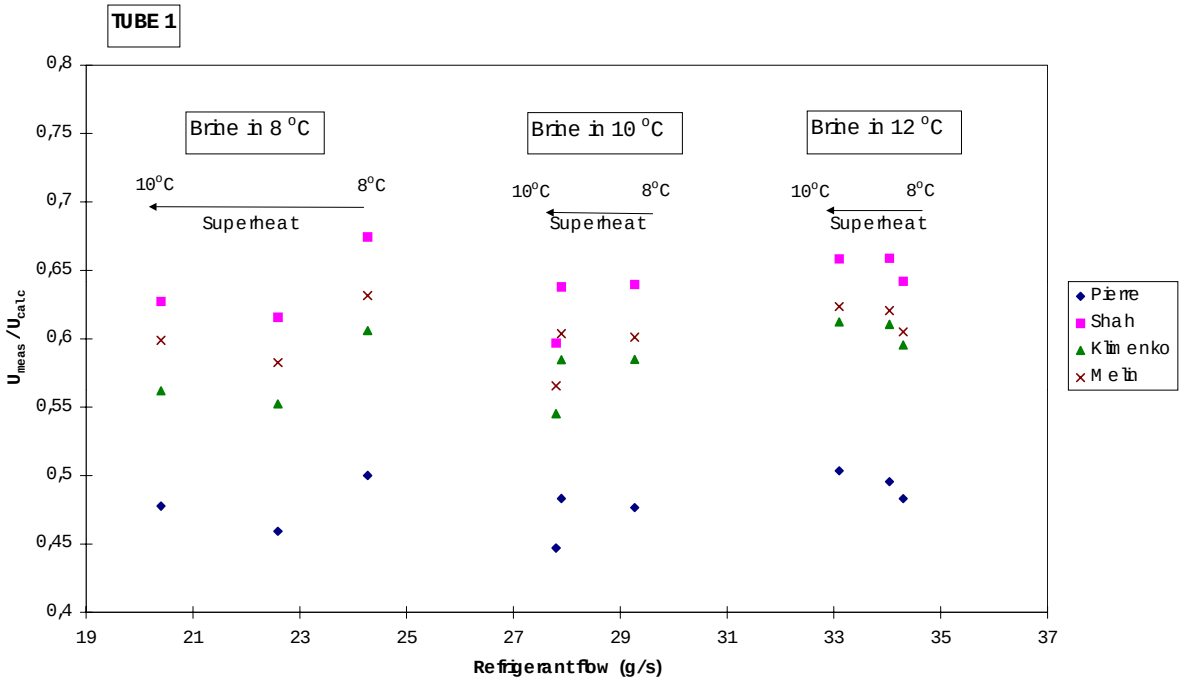

Figure 0-2 Correlation results for measurements with tube 1

7.2.3 Pressure drop - correlation comparison

Measured pressure drops in both tubes were virtually equal in all cases. Therefore the main information achieved from Figure 0-3 and 0-4 is how well the calculated pressure drops coincide with the measured ones.

The correlation from *Chawla* and *Bankoff*, which is mainly used in the Department of Heat and Power Technology, performs very well up to 0.4 bar pressure drop, meaning a deviation not larger than +/- 3% in most cases. At higher pressure drops the deviation increases up to 14%.

Pierre's correlation on the other hand produces better results at higher pressure drops. Over 0.4 bar pressure drop the deviation is not larger than +3%. In the region of lower pressure drops the correlation produces results with a deviation up to +20 %.

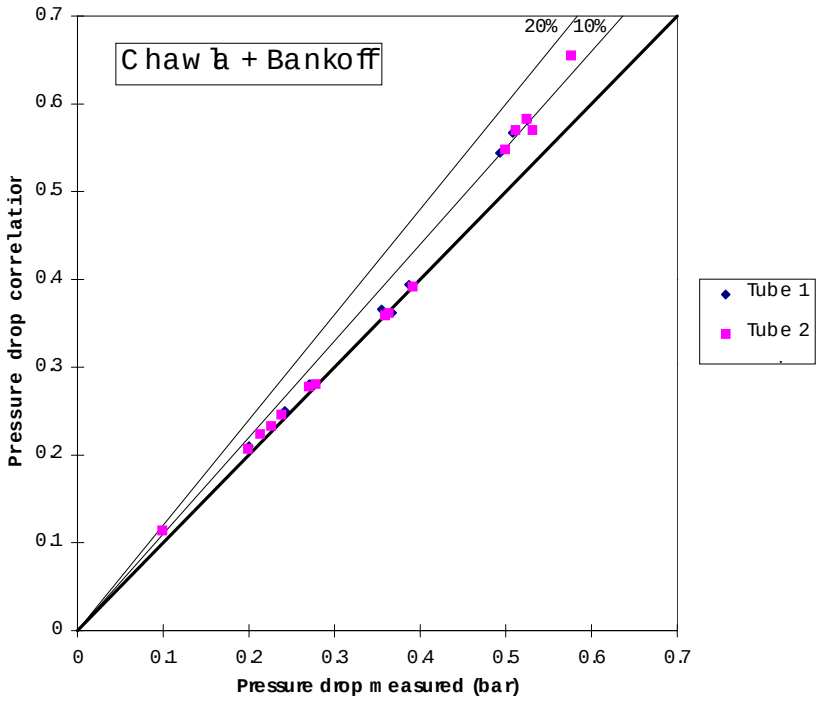

Figure 0-3 Pressure drop correlation from Chawla and Bankoff versus measured data

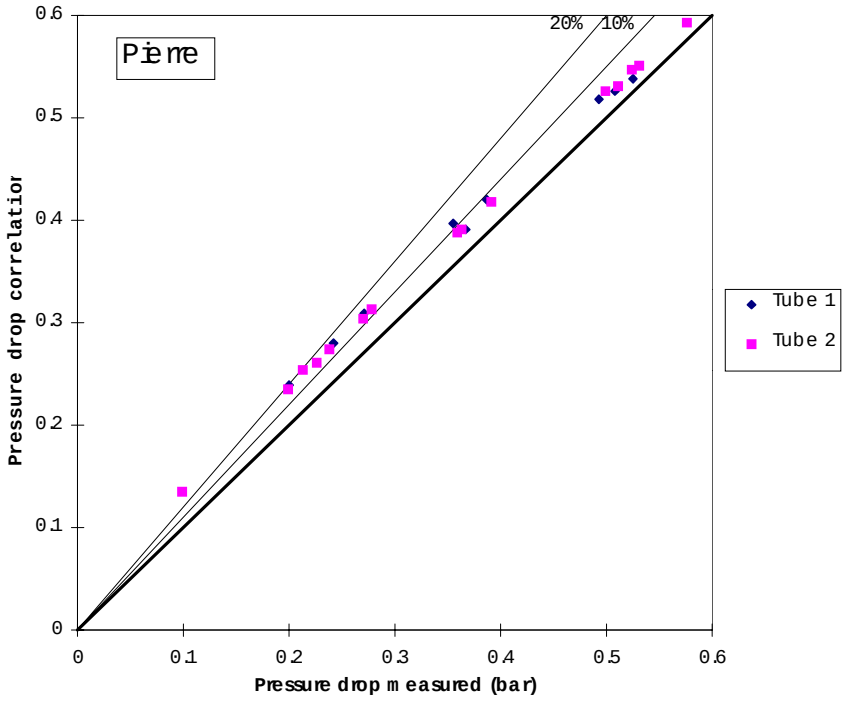

Figure 0-4 Pressure drop correlation from Pierre versus measured data

7.3 Discussion

All the heat transfer correlations were developed in straight smooth tubes and thus it is not surprising that they show deviations when applied to tubes with inserts. The worst performance of Pierre's correlation might be due to the fact that this correlation does not consider the decrease of the heat transfer coefficient at high vapour fractions at all (see Figure 2-3).

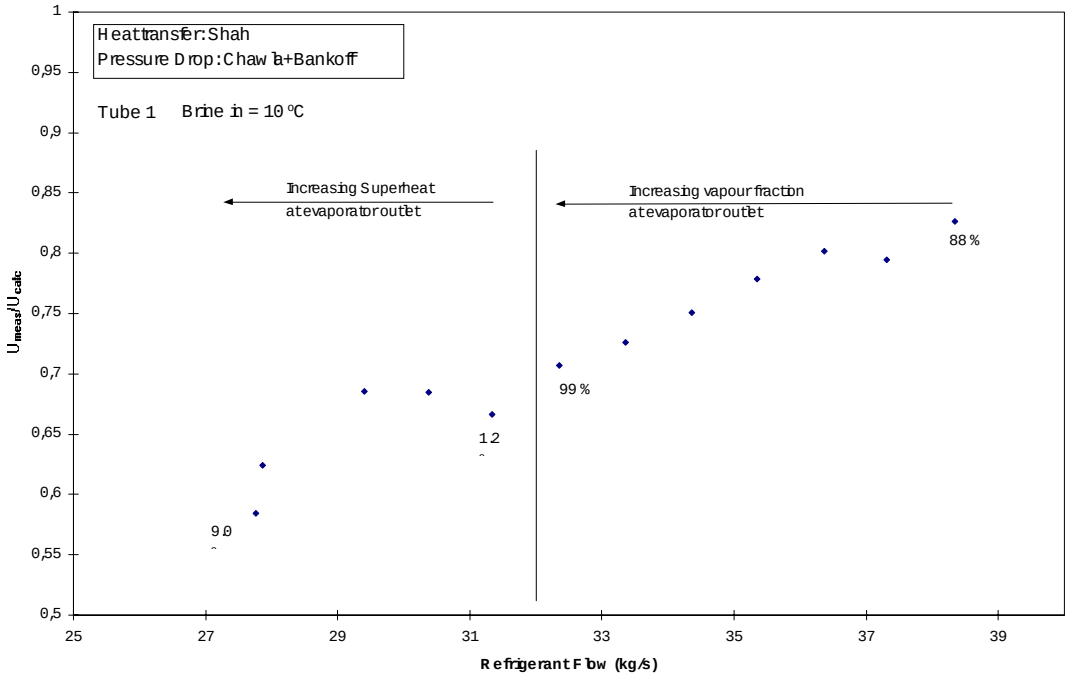

Figure 0-5 Deviation between calculated and measured U-value versus refrigerant flow, at 10 °C brine inlet temperature[2]

For a closer discussion of the correlation results and why they might overestimate the internal heat transfer coefficient, we focus on one specific correlation at a constant brine inlet temperature.

To cover not only conditions where the same amount of superheat occurs but also conditions with two phase flow at the evaporator outlet, the measurement series described in chapter 4.3 is chosen. Figure 0-5 shows from 88% vapour fraction to 9 °C superheat temperature an increasing deviation, meaning an increasing overestimation of the internal heat transfer coefficient.

[2] Note that in this Figure an estimated 7% has been added to the vapour fractions in order to take the error in heat balance discussed in chapter 6.5 into account.

The length of tube where a high vapour fraction occurs might be the decisive factor for the performance of the correlation. As this length increases, the deviation between measured and calculated data increases as well.

Shah's correlation uses the formulation from *Dittus and Boelter* (1985) for heat transfer calculation in the region of high vapour fractions. This addition might be the weak link in the simulation program as it tends to overestimate the heat flux for reasons explained in chapter 2.5. Furthermore the overall heat transfer coefficient in the high vapour fraction region is more dependent on the inner heat transfer and therefore a wrongly estimated heat transfer coefficient here has a bigger influence.

The assumption of *D'Yachov* (1978), where the boundaries between annular, dispersed annular and dispersed flows in ten channel star inserts shift towards smaller vapour fractions compared to smooth tubes, supports the factors discussed above.

Another reason for overestimated heat transfer could be that the correlations use a nucleate boiling contribution for conditions where no nucleate boiling occurs. The 13-14% vapour fraction and the relatively high flows during the measurements are very likely to suppress any nucleate boiling.

8. Conclusions

A comparison of two single evaporator tubes with a ten channel star-shaped insert has been conducted. Afterwards measured data was compared to calculated data using different heat transfer and pressure drop correlations.

The main conclusions are:

8.1 Single tube comparison

- The comparison of different evaporator tubes, even if they use the same kind of insert, has to be carried out for different conditions, since they determine the performance.
- Having covered different flow regions and different heat inputs, this investigation resulted in no general superior behaviour of one of the compared tubes.
- In those conditions close to the ones of the large scale tests a better performance of tube 1 could be confirmed.

- Assumptions about the reasons for the different performance have been made, but could not be proved within this project.

8.2 Numerical comparison

- Using correlations developed for the heat transfer in smooth tubes and adding the specific geometrical parameters of tubes with inserts, leads in the investigated range of conditions to an overestimation of 30 to 50%.
- The pressure drop correlation from *Chawla* (1967) *and Bankoff* (1960) determined the pressure drop within +/- 3% of the measured ones for pressure drops not larger than 0.4 bar. For pressure drops larger than 0.4 bar *Pierre's* (1957) correlation produced results not larger than +3% of the measured data.
- The extended transition area from annular flow to single-phase vapour flow and the correlations' use of a nucleate boiling contribution where no nucleate boiling occurs are likely to be the major causes for the overestimation of heat transfer.

9. Further research

It should be the main purpose of future projects to investigate the flow through the different channels during evaporation condition. A sectional measurement of the heat transfer coefficient like in the work of *Melin* (1996) would be a helpful step on the way to a better understanding of heat transfer in tubes with inserts. In this context one might pay special attention to the distribution to the different channels. The area enhancement (approximately of a factor three) using star-shaped insert is highly dependent on the distribution. Here a comparison with internally finned tubes might be interesting, since the surface enhancement factor is around two, but flow distribution is not a problem.

For all measurements pure HCFC22 has been used. To come even closer to conditions in large scale applications, one of the next investigations should cover the addition of small amounts of oil (0.2-0.3%) to the refrigerant.

Future testing should also consider potential substitute refrigerant fluids.

10. Acknowledgements

I would like to thank Dr. Lennart Vamling for organising my stay at the Department of Heat and Power Technology and for being a supervisor who helped me with many encouraging discussions.

Special thanks to Ulf Stenman for being a friend, helping me with all the practical matters and for teaching me some “Finnish”.

I wish to thank also Eng. Cecilia Gabrielii who’s door always was open and who never hesitated to help.

Prof. Thore Berntsson gave me the opportunity to work at his department. For this I would like to thank him very much.

A sincere word of gratitude goes to Dr. Simon Harvey who corrected my English and with whom I followed King Vasa’s footprints.

Of course I have to thank all the friendly people in the Department of Heat and Power Technology. They made my stay comfortable (thanks Bengt for not hurting me on Tuesday mornings) and compensated for the dark Swedish winter.

Now, reaching the end of my studies, I would like to take the opportunity to thank my dear parents, who always supported me in the most generous way. I wish to let them know how much I appreciate all what they did for me and what is impossible to write down in just a few words.

11. Nomenclature

A	area	m^2
b	Laplace constant	-
C	thermophysical constant	-
Co	convection number	-
c_p	heat capacity	J/(kg K)
d_b	break-off diameter	m
d_i	inner diameter	m
E	enhancement factor of the single-phase forced convection	-
Fr	Froud number	-
G	mass flux	kg/m^2
g	gravitational constant	m/s^2
h	enthalpy	J/kg
h_v	latent heat	J/kg
i_{fg}	latent heat	J/kg
K_f	Pierre's boiling number	-
L	length of evaporator	m
l	length of evaporator	m
$\dot{M}$	mass flow	kg/s
$\dot{m}$	mass flow	kg/s
N_{CB}	convective boiling number	-
Nu	Nusselt number	-
p	pressure	Pa
Pe	Peclét number	-
P_r	reduced pressure	-
$\dot{Q}$	heat rate	W
$\dot{q}$	heat flux	W/m^2
Re	Reynolds number	-
S	nucleate boiling suppression factor	-
T	temperature	K

U	overall heat transfer coefficient	$W/(m^2K)$
w	velocity	m/s
X_{tt}	Martinelli parameter	-
x^*	vapour fraction	-

Greek

α	heat transfer coefficient	$W/(m^2K)$
δ	wall thickness	m
ε	dimensionless number in (2.50)	-
ϕ	two-phase multiplier (pressure)	-
η	dynamic viscosity (in 2.47)	N/(ms)
λ	heat conductivity	W/(mK)
μ	dynamic viscosity	Ns/m^2
ν	kinematic viscosity	m^2/s
ρ	density	kg/m^3
σ	surface tension	N/m
ξ	dimensionless number in (2.36)	-
ψ	two-phase multiplier (heat)	-

Subscripts

a	aussen (outer)
CB	convective boiling
corr	corrected
f	fluid
FC	forced convection
g	gas
h	hydraulic
i	inner
l	liquid
m	two-phase mixture
m	mean value

mod	modified
NB	nucleate boiling
o	outer
v	vapour
w	wall
*	modified

12. References

Bankoff S. G., A Variable Density Single-Fluid Model for Two-Phase with Particular Reference to Steam-Water Flow, *J. Heat Transfer*, Vol. 11 Series B, pp. 265-272, (1960)

Baehr H. D. and Stephan K., Wärme- und Stoffübertragung 2. Auflage, Springer Verlag, (1996).

Chawla J. M., Wärmeübergang und Druckabfall in Waagerechten Rohren bei der Strömung von verdampfenden Kältemitteln, *VDI-Forschungsheft* Vol. 523, pp. 1-36, (1973).

Chawla J. M., Druckverlust in Durchströmten Verdampferrohren, *VDI-Wärmeatlas*, Chapter Lg, (1974).

Collier J. G. and Thome J. R., Convective Boiling and Condensation, Oxford Engineering Series no. 38, Third edition (1994).

Dittus P. W. and Boelter L. M. K., Heat Transfer in Automobile Radiators of the Tubular Type, *International Comm. Heat Mass Transfer*, Vol. 12, pp. 3-22, (1985).

D'Yachkov F. N., Investigation of Heat Transfer and Hydraulics for Boiling of Freon-22 in Internally-Finned Tubes, *Heat Transfer - Soviet Research*, Vol. 10, No. 2, March-April (1978).

ESDU, Forced Convection Heat Transfer in Circular Tubes, Part 1: Correlations for Fully Developed Turbulent Flow - Their Scope and Limitations, *Engineering Science Data*, Item No. 67016, (1967).

Gabrielii C. and Vamling L., Changes in Optimal Design of a Dry-Expansion Evaporator When Replacing R22 with R407 C, *Int. J. Refrig.*, (submitted), (1997).

Gnielinski V., Wärmeübertragung im Konzentrischen Ringspalt, *VDI-Wärmeatlas*, Chapter Gd, (1988).

Kamei A. and Beyerline S. W., A Fundamental Equation For Chlorodifluoromethane (R22), *Proc. ASME 11th Symp. Thermophys. Prop.*, Boulder USA, June (1991).

Klimenko V. V., A Generalised Correlation for Two-Phase Forced Flow Heat Transfer, *Int. Journal of Heat and Mass Transfer*, Vol. 31, No. 3 (1988).

Kubanek G. R. and Miletti D. L., Evaporative Heat Transfer and Pressure Drop Performance of Internally-Finned Tubes with Refigerant 22, Journal of Heat Transfer, Vol. 101, August (1979).

Melin P., Measurements and Modelling of Convective Vaporization for Refigerants in a Horizontal Tube, Ph. D. Thesis, (1996).

Petukhof B. S. and Roizen L. I., *High Temperature 2*, pp. 65-68, (1964).

Pierre B., Strömningsmotstånd vid kokande köldmedier, *Kyltknisk tidskrift*, Dec. (1957).

Pierre B., Värmeövergången vid kokande köldmedier i horisontella rör, *Kyltknisk tidskrift*, (1969).

Shah M. M., A New Correlation for Heat Transfer during Boiling Flow through Pipes, *ASHRAE Trans.* Vol. 82, Part 1 (1982).

Shah M. M., Chart Correlation for Saturated Boiling Heat Transfer: Equations and Further Study, *ASHRAE Trans.* Vol. 8, Part 1 (1982).

Stephan K., *Chem.-Ing.-Technik 34*, pp. 207-212, (1962).

Styushin N. G., Heat Transfer Intensity in Forced Flow Boiling, Heat Transfer and Hydrodynamics, *Izd. Nauka*, Leningrad (1977).

Appendix A - Instrumentation

INSTRUMENT	TYPE	RANGE	INACCURACY
Refrigerant high-pressure pump	Caster MPA 214Cs	- 250 l/h	
Mass flow meter	EXAC Type WX 12	3 - 300 kg/h	< 0.15 % MV
Heat exchanger	Spirec K4F, 304L		
Expansion valve	Bauman microseal		
Brine pump	Grundfos CHI 2-60	- 3,5 m^3/h	
Brine flow meter	Krohne Altometer K 480 AS	0 - 900 l/h	< 0.5 % MV
Magnetic valves	ASCO Type SCE224A4J		
Pt 100	Pentronic		+/- 0.01 K
Quartz thermometer (calibration)	Hewlett-Packard Type 2804 A		+/- 0.01 K
Thermocouples	Type T		+/- 1 % MV
Scanner	Keithley Type KEI - 706		< 1 μV (contact potential)
Multimeter	Keithley 2000		< 1 μV (contact potential)
Abs. Pressure transducer	Setra Systems C280E	0 - 34.5 bar and 0 - 17.2 bar	0.11 % of FS
Diff. Pressure trancducer	Fuji, FKCX34V2	0 - 60 kPa	0.1 % CR

MV : Measured value

FS : Full scale

CR : Calibrated range

Appendix B - Evaporator dimensions

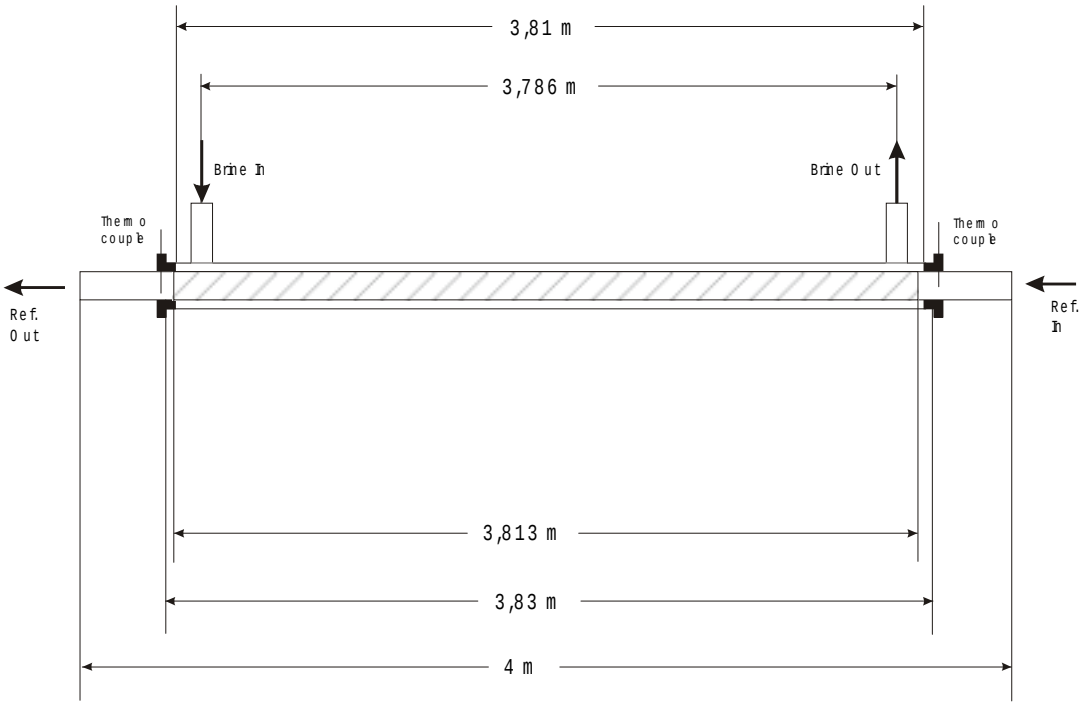

Evaporator Tube		
Length of evaporator tube	4	m
Outer diameter	0,019	m
Inner diameter	0,0174	m
Length of evaporator tube with brine contact	3,81	m
Area evap. tube outside A_{out} (length with brine contact)	0,227	m^2
Internal area	0,196	m^2/m
Length of evaporator insert	3,813	m
Distance between Brine in- and outlet	3,786	m
Length of outer tube	3,83	m

Evaporator cross-section

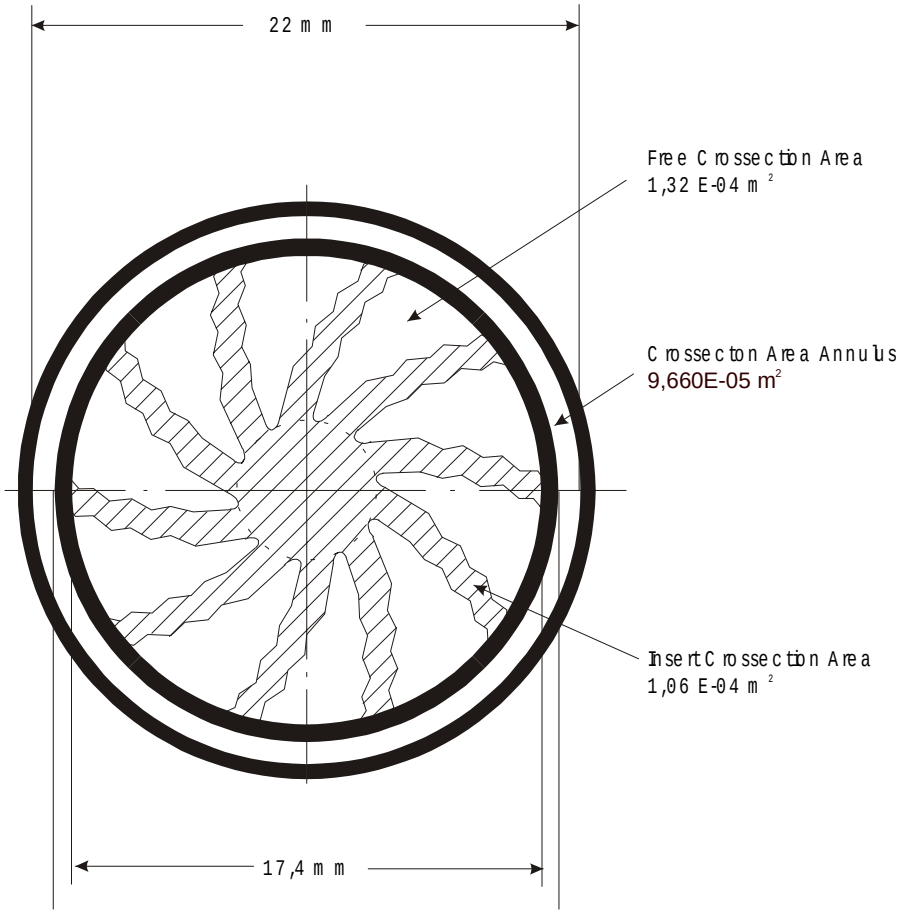

Appendix C - Tables flow/superheat comparison

Experiment 29
Measurements on straight tube with star-shaped insert

Brine Inlet Temperature 12 C !

Tube		**Tube 1**	**Tube 2**	**Tube 2**
			Same Refrigerant flow	**Same Superheat**
This are the measurement results from:		Time 20:36:12 Date 01-20-1998	Time 13:50:30 Date 01-27-1998	Time 16:01:29 Date 01-27-1998
	Unit			
Freonflow average value for the entire reading	kg/s	0,03404	0,03412	0,03508
Temp. before expansionvalve	^{o}C	23,864	23,857	23,846
Pressure before expansionvalve	bar	11,093	11,054	11,053
Temp. Refrigerant in	^{o}C	1,035	1,052	1,182
Pressure at evaporator inlet	bar	5,151	5,151	5,176
Enthalpy Ref. In	J/kg	228 860,000	228 852,000	228 838,000
Vapour Fraction	%	13,550	13,546	13,461
Temp.diff. Refrigerant in and out	^{o}C	5,399	6,039	5,298
Pressure Diff. Ref. in and out	bar	0,508	0,511	0,531
Enthalpy Diff.	J/kg	181 458,000	181 945,000	181 511,000
Temp Refrigerant out	^{o}C	6,434	7,091	6,480
Pressure at evaporarator outlet	bar	4,643	4,641	4,644
Temperature at Dew Point	^{o}C	-2,14	-2,15	-2,13
Superheat Temperature	^{o}C	8,574	9,241	8,610
Enthalpy Ref. Out	kJ/kg	410 318,000	410 797,000	410 349,000
Temp. brine in	^{o}C	12,070	12,058	12,093
Temp.diff. brine in and out	^{o}C	5,224	5,258	5,372
Temp. brine out	^{o}C	6,846	6,801	6,722
Brine Flow	g/s	260,654	260,421	260,394
Brine Velocity	m/s	2,700	2,697	2,697
Re Number		**6 197,101**	**6 191,555**	**6 190,927**
Transfered Heat from Brineside	**W**	**5 732,966**	**5 764,380**	**5 888,882**
Transfered Heat on Refside	**W**	**6 176,781**	**6 207,070**	**6 367,326**
Deviation	%	7,185	7,132	7,514
Transferred Heat from Brineside / $Area_{(outer\ tube)}$	W/m^2	25 255,355	25 393,743	25 942,210
Mean Delta T_{ln} (using dew point temperature)	^{o}C	11,399	11,378	11,326
Overall htc U_m (no concideration of superheat)	**$W/(m^2K)$**	**2 211,421**	**2 227,749**	**2 286,265**
Overall htc U_m (numerical determination)	**$W/(m^2K)$**	**2 640,200**	**2 651,200**	**2 745,540**
Outer heat transfer coefficient α_o	**$W/(m^2K)$**	**9117,159**	**9108,811**	**9113,931**
Inner heat transfer coefficient α_I	**$W/(m^2K)$**	**9588,124**	**9684,676**	**10022,421**

Experiment 19

Measurements on straight tube with star-shaped insert

Brine Inlet Temperature 10 C !

Tube		**Tube 1**	**Tube 2**
			Same Refrigerant flow
This are the measurement results from:		Time 21:55:59 Date 01-16-1998	Time 16:45:57 Date 01-27-1998
	Unit		
Freonflow average value for the entire reading	kg/s	0,0278	0,02776
Temp. before expansionvalve	^{o}C	24,024	23,948
Pressure before expansionvalve	bar	11,060	11,048
Temp. Refrigerant in	^{o}C	-0,129	-0,131
Pressure at evaporator inlet	bar	4,960	4,958
Enthalpy Ref. In	J/kg	229 060,000	228 965,000
Vapour Fraction	%	14,251	14,212
Temp.diff. Refrigerant in and out	^{o}C	6,732	6,464
Pressure Diff. Ref. in and out	bar	0,367	0,359
Enthalpy Diff.	J/kg	181 484,000	181 372,000
Temp Refrigerant out	^{o}C	6,603	6,334
Pressure at evaporarator outlet	bar	4,593	4,599
Temperature at Dew Point	^{o}C	-2,47	-2,43
Superheat Temperature	^{o}C	9,073	8,764
Enthalpy Ref. Out	kJ/kg	410 544,000	410 337,000
Temp. brine in	^{o}C	10,417	10,413
Temp.diff. brine in and out	^{o}C	4,237	4,235
Temp. brine out	^{o}C	6,180	6,178
Brine Flow	g/s	260,664	260,758
Brine Velocity	m/s	2,700	2,701
Re Number		**6 197,349**	**6 199,579**
Transfered Heat from Brineside	**W**	**4 649,163**	**4 649,428**
Transfered Heat on Refside	**W**	**5 044,115**	**5 035,405**
Deviation	%	7,830	7,665
Transferred Heat from Brineside / $Area_{(outer\ tube)}$	W/m^2	20 480,894	20 482,064
Mean Delta T_{ln} (using dew point temperature)	^{o}C	10,628	10,585
Overall htc U_m (no concideration of superheat)	**W/(m^{2}K)**	**1 923,527**	**1 931,512**
Overall htc U_m (numerical determination)	**W/(m^{2}K)**	**2 231,780**	**2 169,690**

Outer heat transfer coefficient α_o	**W/(m^{2}K)**	**9117,531**	**9120,887**

Inner heat transfer coefficient α_I	**W/(m^{2}K)**	**8006,035**	**8047,411**

Experiment 20
Measurements on straight tube with star-shaped insert

Brine Inlet Temperature 8 C !

Tube		**Tube 1**	**Tube 2**	**Tube 2**
			Same Refrigerant flow	**Same Superheat**
This are the measurement results from:		Time 01:44:14 Date 01-17-1998	Time 14:08:21 Date 01-28-1998	Time 21:33:05 Date 01-27-1998
	Unit			
Freonflow average value for the entire reading	kg/s	0,02259	0,02259	0,02140
Temp. before expansionvalve	°C	24,113	24,042	24,035
Pressure before expansionvalve	bar	11,071	11,065	11,071
Temp. Refrigerant in	°C	-0,982	-0,950	-1,152
Pressure at evaporator inlet	bar	4,826	4,847	4,830
Enthalpy Ref. In	J/kg	229 172,000	229 083,000	229 074,000
Vapour Fraction	%	14,736	14,625	14,676
Temp.diff. Refrigerant in and out	°C	7,398	5,990	7,591
Pressure Diff. Ref. in and out	bar	0,242	0,238	0,213
Enthalpy Diff.	J/kg	181 255,000	180 299,000	181 304,000
Temp Refrigerant out	°C	6,416	5,039	6,439
Pressure at evaporarator outlet	bar	4,584	4,609	4,616
Temperature at Dew Point	°C	-2,53	-2,36	-2,32
Superheat Temperature	°C	8,946	7,399	8,759
Enthalpy Ref. Out	kJ/kg	410 427,000	409 382,000	410 378,000
Temp. brine in	°C	8,482	8,463	8,436
Temp.diff. brine in and out	°C	3,399	3,381	3,204
Temp. brine out	°C	5,083	5,083	5,232
Brine Flow	g/s	260,488	261,028	260,381
Brine Velocity	m/s	2,698	2,704	2,697
Re Number		**6 193,166**	**6 205,986**	**6 190,613**
Transfered Heat from Brineside	**W**	**3 727,927**	**3 715,216**	**3 512,069**
Transfered Heat on Refside	**W**	**4 094,753**	**4 073,647**	**3 879,735**
Deviation	%	8,958	8,799	9,477
Transferred Heat from Brineside / $Area_{(outer\ tube)}$	W/m^2	16 422,585	16 366,589	15 471,669
Mean Delta T_{ln} (using dew point temperature)	°C	9,208	9,028	9,060
Overall htc U_m (no concideration of superheat)	**$W/(m^2K)$**	**1 780,156**	**1 809,587**	**1 704,589**
Overall htc U_m (numerical determination)	**$W/(m^2K)$**	**1 941,170**	**2 005,580**	**1 833,720**
Outer heat transfer coefficient α_o	**$W/(m^2K)$**	**9111,237**	**9130,527**	**9100,365**
Inner heat transfer coefficient α_I	**$W/(m^2K)$**	**7265,743**	**7411,755**	**6888,227**

Experiment 21
Measurements on straight tube with star-shaped insert

Brine Inlet Temperature 12 C !

Tube		**Tube 1**	**Tube 2**	**Tube 2**
			Same Refrigerant flow	**Same Superheat**
This are the measurement results from:		Time 16:14:33 Date 01-19-1998	Time 14:06:07 Date 01-28-1998	Time 14:52:13 Date 01-28-1998
	Unit			
Freonflow average value for the entire reading	kg/s	0,0343	0,03429	0,03658
Temp. before expansionvalve	°C	23,907	23,788	23,783
Pressure before expansionvalve	bar	11,063	11,066	11,066
Temp. Refrigerant in	°C	0,866	0,733	1,053
Pressure at evaporator inlet	bar	5,123	5,103	5,155
Enthalpy Ref. In	J/kg	228 914,000	228 765,000	228 759,000
Vapour Fraction	%	13,667	13,654	13,488
Temp.diff. Refrigerant in and out	°C	4,999	6,817	4,815
Pressure Diff. Ref. in and out	bar	0,525	0,524	0,576
Enthalpy Diff.	J/kg	181 087,000	182 491,000	181 285,000
Temp Refrigerant out	°C	5,865	7,550	5,869
Pressure at evaporarator outlet	bar	4,598	4,578	4,579
Temperature at Dew Point	°C	-2,43	-2,57	-2,56
Superheat Temperature	°C	8,295	10,120	8,429
Enthalpy Ref. Out	kJ/kg	410 001,000	411 256,000	410 044,000
Temp. brine in	°C	12,062	12,059	12,117
Temp.diff. brine in and out	°C	5,285	5,298	5,622
Temp. brine out	°C	6,778	6,761	6,495
Brine Flow	g/s	260,638	260,636	260,406
Brine Velocity	m/s	2,700	2,700	2,697
Re Number		**6 196,716**	**6 196,666**	**6 191,203**
Transfered Heat from Brineside	**W**	**5 798,727**	**5 813,100**	**6 163,924**
Transfered Heat on Refside	**W**	**6 212,019**	**6 257,240**	**6 631,101**
Deviation	%	6,653	7,098	7,045
Transferred Heat from Brineside / $Area_{(outer\ tube)}$	W/m^2	25 545,054	25 608,369	27 153,850
Mean Delta T_{ln} (using dew point temperature)	°C	11,651	11,782	11,640
Overall htc U_m (no concideration of superheat)	**$W/(m^2K)$**	**2 188,508**	**2 169,520**	**2 328,399**
Overall htc U_m (numerical determination)	**$W/(m^2K)$**	**2 602,590**	**2 558,260**	**2 850,190**
Outer heat transfer coefficient α_o	**$W/(m^2K)$**	**9116,579**	**9099,692**	**9108,281**
Inner heat transfer coefficient α_I	**$W/(m^2K)$**	**9457,590**	**9355,327**	**10272,692**

Experiment 22

Measurements on straight tube with star-shaped insert

Brine Inlet Temperature 10 C !

Tube		**Tube 1**	**Tube 2**
			Same Refrigerant flow
This are the measurement results from:		Time 17:23:42 Date 01-19-1998	Time 15:48:41 Date 01-28-1998
	Unit		
Freonflow average value for the entire reading	kg/s	0,02927	0,02928
Temp. before expansionvalve	^{o}C	23,987	23,909
Pressure before expansionvalve	bar	11,062	11,061
Temp. Refrigerant in	^{o}C	-0,117	-0,056
Pressure at evaporator inlet	bar	4,962	4,981
Enthalpy Ref. In	J/kg	229 014,000	228 917,000
Vapour Fraction	%	14,223	14,115
Temp.diff. Refrigerant in and out	^{o}C	5,599	5,842
Pressure Diff. Ref. in and out	bar	0,387	0,391
Enthalpy Diff.	J/kg	180 759,000	181 044,000
Temp Refrigerant out	^{o}C	5,482	5,786
Pressure at evaporarator outlet	bar	4,575	4,590
Temperature at Dew Point	^{o}C	-2,59	-2,49
Superheat Temperature	^{o}C	8,072	8,276
Enthalpy Ref. Out	kJ/kg	409 773,000	409 961,000
Temp. brine in	^{o}C	10,117	10,218
Temp.diff. brine in and out	^{o}C	4,440	4,448
Temp. brine out	^{o}C	5,678	5,771
Brine Flow	g/s	260,732	260,436
Brine Velocity	m/s	2,701	2,698
Re Number		**6 198,951**	**6 191,923**
Transfered Heat from Brineside	**W**	**4 873,420**	**4 876,680**
Transfered Heat on Refside	**W**	**5 290,595**	**5 300,887**
Deviation	%	7,885	8,003
Transferred Heat from Brineside / $Area_{(outer\ tube)}$	W/m^2	21 468,812	21 483,171
Mean Delta T_{ln} (using dew point temperature)	^{o}C	10,329	10,325
Overall htc U_m (no concideration of superheat)	**$W/(m^2K)$**	**2 074,679**	**2 076,787**
Overall htc U_m (numerical determination)	**$W/(m^2K)$**	**2 376,530**	**2 396,740**
Outer heat transfer coefficient α_o	**$W/(m^2K)$**	**9119,942**	**9109,366**
Inner heat transfer coefficient α_I	**$W/(m^2K)$**	**8819,795**	**8834,422**

Experiment 23
Measurements on straight tube with star-shaped insert

Brine Inlet Temperature 8 C !

Tube		**Tube 1**	**Tube 2**	**Tube 2**
			Same Refrigerant flow	**Same Superheat**
This are the measurement results from:		Time 17:58:39 Date 01-19-1998	Time 16:14:55 Date 01-28-1998	Time 17:54:15 Date 01-28-1998
	Unit			
Freonflow average value for the entire reading	kg/s	0,02427	0,02428	0,02177
Temp. before expansionvalve	°C	24,076	24,025	24,056
Pressure before expansionvalve	bar	11,058	11,045	11,060
Temp. Refrigerant in	°C	-0,791	-0,728	-1,139
Pressure at evaporator inlet	bar	4,859	4,869	4,804
Enthalpy Ref. In	J/kg	229 125,000	229 060,000	229 100,000
Vapour Fraction	%	14,607	14,572	14,773
Temp.diff. Refrigerant in and out	°C	6,353	4,903	6,681
Pressure Diff. Ref. in and out	bar	0,271	0,270	0,226
Enthalpy Diff.	J/kg	180 679,000	179 719,000	180 710,000
Temp Refrigerant out	°C	5,562	4,175	5,542
Pressure at evaporarator outlet	bar	4,588	4,599	4,578
Temperature at Dew Point	°C	-2,5	-2,43	-2,57
Superheat Temperature	°C	8,062	6,605	8,112
Enthalpy Ref. Out	kJ/kg	409 804,000	408 779,000	409 810,000
Temp. brine in	°C	8,188	8,205	8,152
Temp.diff. brine in and out	°C	3,625	3,591	3,218
Temp. brine out	°C	4,563	4,615	4,934
Brine Flow	g/s	260,601	260,628	260,572
Brine Velocity	m/s	2,699	2,700	2,699
Re Number		**6 195,836**	**6 196,481**	**6 195,145**
Transfered Heat from Brineside	**W**	**3 977,092**	**3 939,876**	**3 530,463**
Transfered Heat on Refside	**W**	**4 385,567**	**4 362,905**	**3 934,958**
Deviation	%	9,314	9,696	10,280
Transferred Heat from Brineside / $Area_{(outer\ tube)}$	W/m^2	17 520,231	17 356,282	15 552,700
Mean Delta T_{ln} (using dew point temperature)	°C	8,751	8,717	9,018
Overall htc U_m (no concideration of superheat)	**$W/(m^2K)$**	**1 998,426**	**1 987,402**	**1 721,496**
Overall htc U_m (numerical determination)	**$W/(m^2K)$**	**2 226,230**	**2 201,170**	**1 863,400**
Outer heat transfer coefficient α_o	**$W/(m^2K)$**	**9115,255**	**9114,243**	**9109,670**
Inner heat transfer coefficient α_I	**$W/(m^2K)$**	**8405,877**	**8346,837**	**6970,827**

Experiment 24

Measurements on straight tube with star-shaped insert

Brine Inlet Temperature 12 C !

Tube		**Tube 1**	**Tube 2**
			Same Refrigerant flow
This are the measurement results from:		Time 18:27:58 Date 01-19-1998	Time 18:42:21 Date 01-28-1998
	Unit		
Freonflow average value for the entire reading	kg/s	0,0331	0,03308
Temp. before expansionvalve	^{o}C	23,928	23,858
Pressure before expansionvalve	bar	11,056	11,060
Temp. Refrigerant in	^{o}C	0,694	0,458
Pressure at evaporator inlet	bar	5,095	5,055
Enthalpy Ref. In	J/kg	228 940,000	228 853,000
Vapour Fraction	%	13,767	13,849
Temp.diff. Refrigerant in and out	^{o}C	7,360	7,720
Pressure Diff. Ref. in and out	bar	0,493	0,499
Enthalpy Diff.	J/kg	182 630,000	182 899,000
Temp Refrigerant out	^{o}C	8,054	8,178
Pressure at evaporarator outlet	bar	4,602	4,556
Temperature at Dew Point	^{o}C	-2,41	-2,71
Superheat Temperature	^{o}C	10,464	10,888
Enthalpy Ref. Out	kJ/kg	411 570,000	411 752,000
Temp. brine in	^{o}C	12,014	12,041
Temp.diff. brine in and out	^{o}C	5,087	5,090
Temp. brine out	^{o}C	6,928	6,951
Brine Flow	g/s	260,680	260,705
Brine Velocity	m/s	2,700	2,700
Re Number		**6 197,727**	**6 198,309**
Transfered Heat from Brineside	**W**	**5 582,291**	**5 587,036**
Transfered Heat on Refside	**W**	**6 043,512**	**6 051,107**
Deviation	%	7,632	7,669
Transferred Heat from Brineside / Area$_{(outer\ tube)}$	W/m^2	24 591,588	24 612,495
Mean Delta T_{ln} (using dew point temperature)	^{o}C	11,697	12,027
Overall htc U_m (no concideration of superheat)	**W/(m^{2}K)**	**2 098,434**	**2 042,685**
Overall htc U_m (numerical determination)	**W/(m^{2}K)**	**2 437,820**	**2 368,310**
Outer heat transfer coefficient α_o	**W/(m^{2}K)**	**9118,100**	**9112,310**
Inner heat transfer coefficient α_I	**W/(m^{2}K)**	**8951,500**	**8646,616**

Sabroe 25

Measurements on straight tube with star-shaped insert

Brine Inlet Temperature 10 C !

Tube		**Tube 1**	**Tube 2**	**Tube 2**
			Same Refrigerant flow	**Same Superheat**
This are the measurement results from:		Time 18:49:00 Date 01-19-1998	Time 19:31:31 Date 02-17-1998	Time 20:33:11 Date 02-17-1998
	Unit			
Freonflow average value for the entire reading	kg/s	0,02829	0,02831	0,02566
Temp. before expansionvalve	^{o}C	24,025	23,915	23,979
Pressure before expansionvalve	bar	11,062	11,065	11,068
Temp. Refrigerant in	^{o}C	-0,167	-0,034	-0,550
Pressure at evaporator inlet	bar	4,954	4,974	4,891
Enthalpy Ref. In	J/kg	229 062,000	228 924,000	229 004,000
Vapour Fraction	%	14,271	14,141	14,445
Temp.diff. Refrigerant in and out	^{o}C	7,162	6,144	7,471
Pressure Diff. Ref. in and out	bar	0,373	0,366	0,311
Enthalpy Diff.	J/kg	181 789,000	181 269,000	181 858,000
Temp Refrigerant out	^{o}C	6,995	6,159	7,008
Pressure at evaporarator outlet	bar	4,581	4,608	4,580
Dew Point Temperature	^{o}C	-2,550	-2,370	-2,550
Superheat	^{o}C	9,545	8,529	9,558
Enthalpy Ref. Out	kJ/kg	410 851,000	410 193,000	410 862,000
Temp. brine in	^{o}C	10,124	10,131	10,209
Temp.diff. brine in and out	^{o}C	4,326	4,318	3,916
Temp. brine out	^{o}C	5,798	5,813	6,293
Brine Flow	g/s	260,647	260,841	260,524
Brine Velocity	m/s	2,700	2,702	2,699
Re Number		**6 196,947**	**6 201,557**	**6 194,013**
Transfered Heat from Brineside	**W**	**4 746,636**	**4 742,072**	**4 295,472**
Transfered Heat on Refside	**W**	**5 143,485**	**5 132,358**	**4 665,687**
Deviation	%	7,716	7,604	7,935
Transferred Heat from Brineside / $Area_{(outer\ tube)}$	W/m^2	20 910,293	20 890,185	18 922,784
Mean Delta T_{ln} (using dew point temperature)	^{o}C	10,361	10,190	10,682
Overall htc U_m (no concideration of superheat)	**$W/(m^2K)$**	**2 014,460**	**2 046,236**	**1 768,226**
Overall htc U_m (numerical determination)	**$W/(m^2K)$**	**2 272,520**	**2 303,658**	**1 896,336**
Outer heat transfer coefficient α_o	**$W/(m^2K)$**	**9116,926**	**9123,863**	**9112,511**
Inner heat transfer coefficient α_I	**$W/(m^2K)$**	**8492,010**	**8662,824**	**7205,086**

Experiment 27

Measurements on straight tube with star-shaped insert

Brine Inlet Temperature 8 C !

Tube		**Tube 1**	**Tube 2**	**Tube 2**
			Same Refrigerant flow	**Same Superheat**
This are the measurement results from:		Time 15:30:14 Date 01-20-1998	Time 13:17:42 Date 01-30-1998	Time 14:28:20 Date 01-30-1998
	Unit			
Freonflow average value for the entire reading	kg/s	0,0204	0,02040	0,01444
Temp. before expansionvalve	°C	24,093	24,086	24,120
Pressure before expansionvalve	bar	11,051	11,056	11,064
Temp. Refrigerant in	°C	-1,278	-1,096	-1,907
Pressure at evaporator inlet	bar	4,777	4,817	4,679
Enthalpy Ref. In	J/kg	229 079,000	229 138,000	229 180,000
Vapour Fraction	%	14,849	14,749	15,218
Temp.diff. Refrigerant in and out	°C	8,487	7,544	9,122
Pressure Diff. Ref. in and out	bar	0,200	0,199	0,099
Enthalpy Diff.	J/kg	181 901,000	181 240,000	181 831,000
Temp Refrigerant out	°C	7,209	6,448	7,215
Pressure at evaporarator outlet	bar	4,593	4,619	4,580
Temperature at Dew Point	°C	-2,47	-2,3	-2,55
Superheat Temperature	°C	9,679	8,748	9,765
Enthalpy Ref. Out	kJ/kg	410 980,000	410 378,000	411 011,000
Temp. brine in	°C	8,197	8,189	8,180
Temp.diff. brine in and out	°C	3,093	3,042	2,148
Temp. brine out	°C	5,105	5,146	6,031
Brine Flow	g/s	260,432	260,784	260,742
Brine Velocity	m/s	2,698	2,701	2,701
Re Number		**6 191,823**	**6 200,204**	**6 199,193**
Transfered Heat from Brineside	**W**	**3 390,814**	**3 340,157**	**2 358,347**
Transfered Heat on Refside	**W**	**3 713,502**	**3 697,706**	**2 625,611**
Deviation	%	8,690	9,669	10,179
Transferred Heat from Brineside / $Area_{(outer\ tube)}$	W/m^2	14 937,506	14 714,348	10 389,193
Mean Delta T_{ln} (using dew point temperature)	°C	9,033	8,881	9,616
Overall htc U_m (no concideration of superheat)	**$W/(m^2K)$**	**1 650,590**	**1 653,794**	**1 078,450**
Overall htc U_m (numerical determination)	**$W/(m^2K)$**	**1 746,350**	**1 764,220**	**1 084,900**
Outer heat transfer coefficient α_o	**$W/(m^2K)$**	**9109,215**	**9120,611**	**9120,307**
Inner heat transfer coefficient α_I	**$W/(m^2K)$**	**6620,248**	**6634,108**	**4016,666**

Appendix D - Tables superheat starting point

Flow 29		**Tube 1**	**Tube 2**
This are the measurement results from:	Unit	Time 17:47:34 Date 01-21-1998	Time 16:34:32 Date 01-30-1998
Freonflow average value for the entire reading	kg/s	0,02940	0,02936
Temperature before expansionvalve	^{o}C	24,025	23,932
Pressure before expansionvalve	bar	11,055	11,056
Temp. refrigerant in	^{o}C	0,465	0,143
Pressure at evaporator inlet	bar	5,057	5,007
Enthalpy refrigerant in	J/kg	229 062,000	228 945,000
Vapour fraction	%	13,945	14,046
Temp.diff. refrigerant in and out	^{o}C	5,096	5,719
Pressure diff. refrigerant in and out	bar	0,363	0,389
Enthalpy diff.	J/kg	180 519,000	181 012,000
Temp refrigerant out	^{o}C	5,562	5,862
Pressure at evaporarator outlet	bar	4,694	4,618
Temperatur dew point	^{o}C	-1,810	-2,300
Superheat temperature	^{o}C	7,372	8,162
Enthalpy refrigerant out	kJ/kg	409 581,000	409 957,000
Temp. brine in	^{o}C	10,161	10,209
Temp.diff. brine in and out	^{o}C	4,426	4,421
Temp. brine out	^{o}C	5,735	5,789
Brine flow	kg/s	260,581	260,572
Brine velocity	m/s	2,699	2,699
Re number		**6 195,373**	**6 195,156**
Transferred heat from brine side	**W**	**4 855,839**	**4 849,341**
Transferred heat on refrigerant side	**W**	**5 307,148**	**5 315,178**
Deviation	%	8,504	8,764
Transferred heat from brine side / area$_{(outer\ tube)}$	W/m^2	21 391,360	21 362,734
Mean ΔT_{ln}	^{o}C	9,588	10,139
Overall htc U_m	**W/(m^{2}K)**	**2 230,944**	**2 107,039**

Outer heat transfer coefficient α_o	**W/(m^{2}K)**	**9114,558**	**9114,232**

Inner heat transfer coefficient α_I	**W/(m^{2}K)**	**9701,092**	**9000,388**

Flow 30		**Tube 1**	**Tube 2**
This are the measurement results from:		Time 17:17:20 Date 01-21-1998	Time 17:06:14 Date 01-30-1998
	Unit		
Freonflow average value for the entire reading	kg/s	0,03038	0,03036
Temperature before expansionvalve	^{o}C	23,990	23,923
Pressure before expansionvalve	bar	11,064	11,063
Temp. refrigerant in	^{o}C	0,757	0,508
Pressure at evaporator inlet	bar	5,105	5,065
Enthalpy refrigerant in	J/kg	229 018,000	228 934,000
Vapour fraction	%	13,772	13,857
Temp.diff. refrigerant in and out	^{o}C	2,323	4,525
Pressure diff. refrigerant in and out	bar	0,394	0,401
Enthalpy diff.	J/kg	178 725,000	180 327,000
Temp refrigerant out	^{o}C	3,080	5,033
Pressure at evaporarator outlet	bar	4,711	4,664
Temperatur dew point	^{o}C	-1,700	-2,000
Superheat temperature	^{o}C	4,780	7,033
Enthalpy refrigerant out	kJ/kg	407 743,000	409 261,000
Temp. brine in	^{o}C	10,145	10,120
Temp.diff. brine in and out	^{o}C	4,553	4,586
Temp. brine out	^{o}C	5,592	5,534
Brine flow	kg/s	260,745	259,993
Brine velocity	m/s	2,701	2,693
Re number		**6 199,262**	**6 181,391**
Transferred heat from brine side	**W**	**4 998,215**	**5 019,239**
Transferred heat on refrigerant side	**W**	**5 429,044**	**5 475,148**
Deviation	%	7,936	8,327
Transferred heat from brine side / area$_{(outer\ tube)}$	W/m^2	22 018,569	22 111,187
Mean ΔT_{ln}	^{o}C	9,385	9,646
Overall htc U_m	**W/(m^{2}K)**	**2 346,155**	**2 292,201**

Outer heat transfer coefficient α_o	**W/(m^{2}K)**	**9120,411**	**9093,510**

Inner heat transfer coefficient α_I	**W/(m^{2}K)**	**10373,426**	**10064,786**

Flow 31		**Tube 1**	**Tube 2**
This are the measurement results from:		Time 17:01:52 Date 01-21-1998	Time 17:37:24 Date 01-30-1998
	Unit		
Freonflow average value for the entire reading	kg/s	0,03134	0,03132
Temperature before expansionvalve	^{o}C	23,978	23,907
Pressure before expansionvalve	bar	11,064	11,076
Temp. refrigerant in	^{o}C	0,809	0,395
Pressure at evaporator inlet	bar	5,114	5,043
Enthalpy refrigerant in	J/kg	229 003,000	228 914,000
Vapour fraction	%	13,737	13,917
Temp.diff. refrigerant in and out	^{o}C	1,365	3,773
Pressure diff. refrigerant in and out	bar	0,345	3,773
Enthalpy diff.	J/kg	163 304,000	179 812,000
Temp refrigerant out	^{o}C	-0,556	4,169
Pressure at evaporarator outlet	bar	4,700	4,622
Temperatur dew point	^{o}C	-1,770	-2,28
Superheat temperature	^{o}C	1,214	6,449
Enthalpy refrigerant out	kJ/kg	405 115,000	408 726,000
Temp. brine in	^{o}C	10,098	10,130
Temp.diff. brine in and out	^{o}C	4,663	4,700
Temp. brine out	^{o}C	5,436	5,430
Brine flow	kg/s	260,751	260,654
Brine velocity	m/s	2,701	2,700
Re number		**6 199,419**	**6 197,111**
Transferred heat from brine side	**W**	**5 118,322**	**5 157,214**
Transferred heat on refrigerant side	**W**	**5 118,347**	**5 631,172**
Deviation	%		8,417
Transferred heat from brine side / area$_{(outer\ tube)}$	W/m^2	22 547,673	22 719,006
Mean ΔT_{ln}	^{o}C	9,344	9,874
Overall htc U_m	**W/(m^{2}K)**	**2 413,103**	**2 300,879**
Outer heat transfer coefficient α_o	**W/(m^{2}K)**	**9120,647**	**9117,173**
Inner heat transfer coefficient α_I	**W/(m^{2}K)**	**10775,828**	**10106,910**

Flow 32		**Tube 1**	**Tube 2**
This are the measurement results from:		Time 16:36:38 Date 01-21-1998	Time 18:09:08 Date 01-30-1998
	Unit		
Freonflow average value for the entire reading	kg/s	0,03235	0,03238
Temperature before expansionvalve	^{o}C	23,963	23,865
Pressure before expansionvalve	bar	11,058	11,062
Temp. refrigerant in	^{o}C	0,963	0,526
Pressure at evaporator inlet	bar	5,139	5,065
Enthalpy refrigerant in	J/kg	228 984,000	228 862,000
Vapour fraction	%	13,648	13,821
Temp.diff. refrigerant in and out	^{o}C	2,625	3,193
Pressure diff. refrigerant in and out	bar	0,426	0,447
Enthalpy diff.	J/kg	160 588,000	179 547,000
Temp refrigerant out	^{o}C	-1,661	3,719
Pressure at evaporarator outlet	bar	4,713	4,618
Vapour fraction outlet	%	92,880	
Temperatur dew point	^{o}C		-2,3
Superheat temperature	^{o}C		6,019
Enthalpy refrigerant out	kJ/kg	389 572,000	408 409,000
Temp. brine in	^{o}C	10,132	10,108
Temp.diff. brine in and out	^{o}C	4,734	4,852
Temp. brine out	^{o}C	5,398	5,256
Brine flow	kg/s	260,646	260,544
Brine velocity	m/s	2,700	2,699
Re number		**6 196,902**	**6 194,498**
Transferred heat from brine side	**W**	**5 195,024**	**5 322,387**
Transferred heat on refrigerant side	**W**	**5 195,014**	**5 812,931**
Transferred heat from brine side / area$_{(outer\ tube)}$	W/m^2	22 885,568	23 446,640
Mean ΔT_{ln}	^{o}C	7,523	9,782
Overall htc U_m	**W/(m^{2}K)**	**3 042,020**	**2 396,806**

Outer heat transfer coefficient α_o	**W/(m^{2}K)**	**9116,858**	**9113,241**

Inner heat transfer coefficient α_I	**W/(m^{2}K)**	**14992,884**	**10680,209**

Flow 33		**Tube 1**	**Tube 2**
This are the measurement results from:		Time 16:17:54 Date 01-21-1998	Time 18:26:12 Date 01-30-1998
	Unit		
Freonflow average value for the entire reading	kg/s	0,03336	0,03335
Temperature before expansionvalve	^{o}C	23,928	23,870
Pressure before expansionvalve	bar	11,063	11,069
Temp. refrigerant in	^{o}C	1,074	0,601
Pressure at evaporator inlet	bar	5,156	5,078
Enthalpy refrigerant in	J/kg	228 945,000	228 868,000
Vapour fraction	%	13,558	13,783
Temp.diff. refrigerant in and out	^{o}C	2,911	1,055
Pressure diff. refrigerant in and out	bar	0,345	0,461
Enthalpy diff.	J/kg	157 478,000	177 986,000
Temp refrigerant out	^{o}C	-1,706	1,572
Pressure at evaporarator outlet	bar	4,708	4,617
Vapour fraction outlet	%	91,361	
Temperatur dew point	^{o}C		-2,31
Superheat temperature	^{o}C		3,882
Enthalpy refrigerant out	kJ/kg	386 423,000	406 854,000
Temp. brine in	^{o}C	10,125	10,098
Temp.diff. brine in and out	^{o}C	4,787	4,949
Temp. brine out	^{o}C	5,338	5,149
Brine flow	kg/s	260,692	260,670
Brine velocity	m/s	2,700	2,700
Re number		**6 198,012**	**6 197,477**
Transferred heat from brine side	**W**	**5 253,647**	**5 431,170**
Transferred heat on refrigerant side	**W**	**5 253,616**	**5 935,881**
Deviation	%		8,503
Transferred heat from brine side / area$_{(outer\ tube)}$	W/m^2	23 143,818	23 925,861
Mean ΔT_{ln}	^{o}C	7,415	9,725
Overall htc U_m	**W/(m^{2}K)**	**3 121,083**	**2 460,325**
Outer heat transfer coefficient α_o	**W/(m^{2}K)**	**9118,529**	**9124,135**
Inner heat transfer coefficient α_I	**W/(m^{2}K)**	**15583,912**	**11063,036**

Flow 34		**Tube 1**	**Tube 2**
This are the measurement results from:		Time 15:49:02 Date 01-21-1998	Time 18:51:50 Date 01-30-1998
	Unit		
Freonflow average value for the entire reading	kg/s	0,03436	0,03440
Temperature before expansionvalve	^{o}C	23,916	23,833
Pressure before expansionvalve	bar	11,068	11,045
Temp. refrigerant in	^{o}C	1,302	0,742
Pressure at evaporator inlet	bar	5,196	5,102
Enthalpy refrigerant in	J/kg	228 925,000	228 822,000
Vapour fraction	%	13,442	13,683
Temp.diff. refrigerant in and out	^{o}C	2,965	3,088
Pressure diff. refrigerant in and out	bar	0,345	0,474
Enthalpy diff.	J/kg	152 447,000	161 803,000
Temp refrigerant out	^{o}C	-1,532	-1,974
Pressure at evaporarator outlet	bar	4,735	4,628
Vapour fraction outlet	%	88,824	93,503
Enthalpy refrigerant out	kJ/kg	381 372,000	390 625,000
Temp. brine in	^{o}C	10,128	10,120
Temp.diff. brine in and out	^{o}C	4,773	5,074
Temp. brine out	^{o}C	5,355	5,046
Brine flow	kg/s	260,718	260,596
Brine velocity	m/s	2,701	2,699
Re number		**6 198,628**	**6 195,732**
Transferred heat from brine side	**W**	**5 239,040**	**5 566,781**
Transferred heat on refrigerant side	**W**	**5 237,321**	**5 566,790**
Transferred heat from brine side / area$_{(outer\ tube)}$	W/m^2	23 079,472	24 523,265
Mean ΔT_{ln}	^{o}C	7,199	7,540
Overall htc U_m	**W/(m^{2}K)**	**3 205,802**	**3 252,288**

Outer heat transfer coefficient α_o	**W/(m^{2}K)**	**9119,456**	**9115,098**

Inner heat transfer coefficient α_I	**W/(m^{2}K)**	**16235,379**	**16605,704**

Flow 35		**Tube 1**	**Tube 2**
This are the measurement results from:		Time 18:09:39 Date 01-21-1998	Time 19:14:45 Date 01-30-1998
	Unit		
Freonflow average value for the entire reading	kg/s	0,03535	0,03539
Temperature before expansionvalve	^{o}C	23,892	23,794
Pressure before expansionvalve	bar	11,060	11,052
Temp. refrigerant in	^{o}C	1,448	1,063
Pressure at evaporator inlet	bar	5,220	5,164
Enthalpy refrigerant in	J/kg	228 895,000	228 773,000
Vapour fraction	%	13,351	13,466
Temp.diff. refrigerant in and out	^{o}C	3,050	3,104
Pressure diff. refrigerant in and out	bar	0,345	0,479
Enthalpy diff.	J/kg	149 185,000	159 372,000
Temp refrigerant out	^{o}C	-1,457	-1,974
Pressure at evaporarator outlet	bar	4,747	4,685
Vapour fraction outlet	%	87,258	92,226
Enthalpy refrigerant out	kJ/kg	378 080,000	388 145,000
Temp. brine in	^{o}C	10,141	10,172
Temp.diff. brine in and out	^{o}C	4,807	5,139
Temp. brine out	^{o}C	5,334	5,033
Brine flow	kg/s	260,591	260,696
Brine velocity	m/s	2,699	2,700
Re number		**6 195,601**	**6 198,105**
Transferred heat from brine side	**W**	**5 273,754**	**5 640,322**
Transferred heat on refrigerant side	**W**	**5 273,737**	**5 640,280**
Transferred heat from brine side / area$_{(outer\ tube)}$	W/m^2	23 232,398	24 847,232
Mean ΔT_{ln}	^{o}C	7,053	7,311
Overall htc U_m	**W/(m^{2}K)**	**3 293,905**	**3 398,520**
Outer heat transfer coefficient α_o	**W/(m^{2}K)**	**9114,901**	**9118,668**
Inner heat transfer coefficient α_I	**W/(m^{2}K)**	**16938,635**	**17792,075**

Flow 36		**Tube 1**	**Tube 2**
This are the measurement results from:	Unit	Time 18:23:24 Date 01-21-1998	Time 20:03:52 Date 01-30-1998
Freonflow average value for the entire reading	kg/s	0,03636	0,03639
Temperature before expansionvalve	^{o}C	23,870	23,788
Pressure before expansionvalve	bar	11,061	11,054
Temp. refrigerant in	^{o}C	1,571	1,126
Pressure at evaporator inlet	bar	5,241	5,159
Enthalpy refrigerant in	J/kg	228 993,000	228 765,000
Vapour fraction	%	13,334	13,478
Temp.diff. refrigerant in and out	^{o}C	3,150	3,243
Pressure diff. refrigerant in and out	bar	0,345	0,501
Enthalpy diff.	J/kg	146 560,000	157 580,000
Temp refrigerant out	^{o}C	-1,438	-2,043
Pressure at evaporarator outlet	bar	4,749	4,657
Vapour fraction outlet	%	86,029	91,392
Enthalpy refrigerant out	kJ/kg	375 553,000	386 345,000
Temp. brine in	^{o}C	10,146	10,186
Temp.diff. brine in and out	^{o}C	4,854	5,232
Temp. brine out	^{o}C	5,292	4,955
Brine flow	kg/s	260,758	260,347
Brine velocity	m/s	2,701	2,697
Re number		**6 199,574**	**6 189,809**
Transferred heat from brine side	**W**	**5 328,507**	**5 734,300**
Transferred heat on refrigerant side	**W**	**5 328,523**	**5 734,333**
Transferred heat from brine side / area$_{(outer\ tube)}$	W/m^2	23 473,600	25 261,234
Mean ΔT_{ln}	^{o}C	6,924	7,233
Overall htc U_m	**W/(m^{2}K)**	**3 390,096**	**3 492,339**
Outer heat transfer coefficient α_o	**W/(m^{2}K)**	**9120,879**	**9106,184**
Inner heat transfer coefficient α_I	**W/(m^{2}K)**	**17719,335**	**18603,951**

Flow 37		**Tube 1**	**Tube 2**
This are the measurement results from:	Unit	Time 18:32:19 Date 01-21-1998	Time 20:17:08 Date 01-30-1998
Freonflow average value for the entire reading	kg/s	0,03731	0,03731
Temperature before expansionvalve	^{o}C	23,821	23,709
Pressure before expansionvalve	bar	11,080	11,077
Temp. refrigerant in	^{o}C	1,589	1,186
Pressure at evaporator inlet	bar	5,244	5,183
Enthalpy refrigerant in	J/kg	228 807,000	228 667,000
Vapour fraction	%	13,233	13,355
Temp.diff. refrigerant in and out	^{o}C	3,261	3,313
Pressure diff. refrigerant in and out	bar	0,345	0,510
Enthalpy diff.	J/kg	142 760,000	152 630,000
Temp refrigerant out	^{o}C	-1,531	-1,948
Pressure at evaporarator outlet	bar	4,738	4,672
Vapour fraction outlet	%	84,111	88,926
Enthalpy refrigerant out	kJ/kg	371 567,000	381 297,000
Temp. brine in	^{o}C	10,122	10,170
Temp.diff. brine in and out	^{o}C	4,858	5,192
Temp. brine out	^{o}C	5,264	4,978
Brine flow	kg/s	260,441	260,550
Brine velocity	m/s	2,698	2,699
Re number		**6 192,047**	**6 194,638**
Transferred heat from brine side	**W**	**5 326,607**	**5 695,179**
Transferred heat on refrigerant side	**W**	**5 326,277**	**5 695,173**
Transferred heat from brine side / area$_{(outer\ tube)}$	W/m^2	23 465,227	25 088,893
Mean ΔT_{ln}	^{o}C	6,914	7,166
Overall htc U_m	**W/(m^{2}K)**	**3 393,794**	**3 501,134**

Outer heat transfer coefficient α_o	**W/(m^{2}K)**	**9112,325**	**9115,670**

Inner heat transfer coefficient α_I	**W/(m^{2}K)**	**17760,000**	**18667,928**

Flow 38		**Tube 1**	**Tube 2**
This are the measurement results from:	Unit	Time 19:07:56 Date 01-21-1998	Time 22:04:54 Date 01-30-1998
Freonflow average value for the entire reading	kg/s	0,03834	0,03837
Temperature before expansionvalve	^{o}C	23,794	23,734
Pressure before expansionvalve	bar	11,064	11,044
Temp. refrigerant in	^{o}C	1,744	1,165
Pressure at evaporator inlet	bar	5,270	5,173
Enthalpy refrigerant in	J/kg	228 773,000	228 698,000
Vapour fraction	%	13,135	13,401
Temp.diff. refrigerant in and out	^{o}C	3,328	3,471
Pressure diff. refrigerant in and out	bar	0,519	0,536
Enthalpy diff.	J/kg	139 112,000	153 282,000
Temp refrigerant out	^{o}C	-1,453	-2,154
Pressure at evaporarator outlet	bar	4,751	4,637
Vapour fraction outlet	%	82,304	89,307
Enthalpy refrigerant out	kJ/kg	367 885,000	381 980,000
Temp. brine in	^{o}C	10,119	10,177
Temp.diff. brine in and out	^{o}C	4,863	5,360
Temp. brine out	^{o}C	5,256	4,817
Brine flow	kg/s	260,514	260,609
Brine velocity	m/s	2,698	2,699
Re number		**6 193,775**	**6 196,034**
Transferred heat from brine side	**W**	**5 334,069**	**5 881,079**
Transferred heat on refrigerant side	**W**	**5 334,035**	**5 881,058**
Transferred heat from brine side / area$_{(outer\ tube)}$	W/m^2	23 498,100	25 907,838
Mean ΔT_{ln}	^{o}C	6,759	7,132
Overall htc U_m	**W/(m^{2}K)**	**3 476,420**	**3 632,484**

Outer heat transfer coefficient α_o	**W/(m^{2}K)**	**9112,153**	**9115,552**

Inner heat transfer coefficient α_I	**W/(m^{2}K)**	**18459,315**	**19832,418**